Kinetics of Intramolecular Charge Transfer with *N*-Phenylpyrrole in Alkyl Cyanides

Toshitada Yoshihara,[†,‡] Sergey I. Druzhinin,[†] Attila Demeter,[†,§] Nikolaus Kocher,[||] Dietmar Stalke,[||] and Klaas A. Zachariasse*[,†]

Max-Planck-Institut für biophysikalische Chemie, Spektroskopie und Photochemische Kinetik, 37070 Göttingen, Germany, Institute of Chemistry, Chemical Research Center, Hungarian Academy of Sciences, P.O. Box 17, 1525 Budapest, Hungary, and Institut für Anorganische Chemie, Universität Würzburg, Am Hubland, 97074 Würzburg, Germany

Received: July 30, 2004; In Final Form: November 3, 2004

For the electron acceptor/donor molecule *N*-phenylpyrrole (PP), the fast intramolecular charge transfer (ICT) reaction accompanied by dual fluorescence from a locally excited (LE) and an ICT state is investigated in alkyl cyanide solvents as a function of temperature. After a comparison of the X-ray crystal structure of PP with calculations from the literature, absorption and fluorescence spectra of PP in a series of solvents over a wide polarity range are discussed. ICT with PP strongly depends on solvent polarity and starts to appear in solvents more polar than diethyl ether. From an analysis of the ICT/LE fluorescence quantum yield ratio Φ'(ICT)/Φ(LE), approximate data for the change in enthalpy $-\Delta H$ of the ICT reaction of PP are obtained, ranging from 9 kJ/mol in acetonitrile (MeCN) to 4 kJ/mol in *n*-butyl cyanide (BuCN). From ICT and LE fluorescence decays of PP measured as a function of temperature, the forward ($E_a = 9$ kJ/mol in ethyl cyanide (EtCN) and 6 kJ/mol in MeCN) and backward ($E_d = 16$ kJ/mol in EtCN and MeCN) ICT reaction barriers are determined. From these data, $-\Delta H$ (7 kJ/mol (EtCN); 10 kJ/mol (MeCN)) is calculated, in good agreement with the results coming from Φ'(ICT)/Φ(LE). The data for E_a show that the forward ICT barrier becomes smaller with increasing solvent polarity, whereas the absence of change for E_d comes from the compensating increase of $-\Delta H$. Both observations are indicative of a late transition state for the LE → ICT reaction. For PP in EtCN and MeCN, the ICT radiative rate constant k'_f(ICT) increases with temperature. This is caused by the ICT low transition dipole moment and hence does not contain information on the molecular structure (twisted or planar) of the ICT state. The fast ICT observed with PP supports our previous conclusion, based on a comparison of PP with its planarized derivative fluorazene, that the pyrrole and phenyl moieties in the ICT state of PP are coplanar and possess substantial electronic coupling.

Introduction

From the broadening of the fluorescence spectrum of *N*-phenylpyrrole (PP) in the strongly polar solvent acetonitrile (MeCN) at room temperature, attributed to the appearance of a red-shifted additional band, it has been deduced that this molecule undergoes intramolecular charge transfer (ICT).[1−4] With PP in the protic solvents ethanol and *n*-butanol, a less pronounced long-wavelength spectral broadening was reported.[4] The additional band was assumed to have a perpendicularly twisted intramolecular charge transfer (TICT) structure.[1,3,4] Such a dual fluorescence is not observed with PP in nonpolar alkane solvents[1,4,5] nor in the slightly polar diethyl ether,[5] in which solvents the emission spectrum consists of a single band originating from the locally excited (LE) state. Recently, the photostationary fluorescence behavior of PP was investigated in a large range of solvents spanning the polarity scale, from perfluoromethylcyclohexane to methanol.[5] It was established by solvatochromic and thermochromic analysis that the red-shifted second emission band comes from an ICT state, with a dipole moment of around 13 D, much larger than the 2 D value determined for the LE state.[5]

From the similarity of the ICT and LE fluorescence of PP and its planar rigidized derivative fluorazene (FPP), it has been concluded that the ICT state of both molecules has a planar structure.[6] Such an effectively planar structure of the ICT state has also been reported for 1-*tert*-butyl-6-cyano-1,2,3,4-tetrahydroquinoline[7] (NTC6) and 4-(diisopropylamino)benzonitrile[8] (DIABN).

Information on the molecular structure of PP in the electronic ground state has come from photoelectron spectra (PES)[1] and dipole moment measurements.[3] A crystal structure has not been reported in the literature but will be presented here. From the photoelectron spectrum of PP, a mean twist angle between the pyrrole and phenyl moieties of 32° with a large uncertainty range (+17°/−32°) was determined for ground state PP in the gas phase.[1] This value should be compared with the result of ground state dipole moment measurements, from which a mean twist angle of 42° was obtained for PP.[3,9,10] It was, however, concluded from the PES results that PP either is only slightly twisted or possesses a rather broad distribution of the rotational angles centered around the planar conformation.[1] In support of this conclusion, an investigation of ^{13}C NMR chemical shifts in phenyl-substituted azoles indicates that PP is practically planar in the ground state.[4,11,12] Within the context of the TICT hypothesis,[13] it was assumed that the closer the initial twist angle

* Corresponding author. Fax: +49-551-201-1501. E-mail: kzachar@gwdg.de.
† Max-Planck-Institut für biophysikalische Chemie.
‡ Present address: Department of Chemistry, Gunma University, Kiryu, Gunma 376-8515, Japan.
§ Hungarian Academy of Sciences.
|| Universität Würzburg.

10.1021/jp046586j CCC: $30.25
Published on Web 02/08/2005

is to its final value of 90°, the faster will be the TICT population kinetics.[1] This assumption of the essential importance of the ground state twist angle for the efficiency of the ICT reaction does not take into account that the LE state and not the S_0 ground state is the precursor of the final relaxed ICT state.[14]

More precise structural information on PP in the S_0 state as well as in the S_1 state comes from electronic spectra of jet-cooled molecules.[15] The most stable conformation of S_0 was found to have a phenyl/pyrrole twist angle of 38.7°, whereas a somewhat smaller dihedral angle of 19.8° was obtained for S_1. It was concluded from these experiments that upon excitation to S_1 it becomes more difficult to twist the two moieties in PP. The barrier height to reach a planar conformation was reduced from 5.47 kJ/mol in S_0 to 1.26 kJ/mol in S_1, whereas the barrier at the perpendicular conformation increased from 8.96 kJ/mol (S_0) to 18.26 kJ/mol (S_1). The conclusion that no indication for a twisted intramolecular charge transfer (TICT), or other ICT state, appeared on the shape of the S_1 torsional potential is in agreement with the presence of dual fluorescence with PP in strongly polar solvents only, as mentioned above. These results therefore refer to the LE state and have no direct implication for the lowest-energy equilibrium structure of the ICT state. PP was also studied in a supersonic jet with and without acetonitrile clusters, as well as in an argon/acetonitrile matrix at 14−30 K.[16−18] For PP in the jet, only a single LE emission is observed, regardless of the cluster size, whereas PP in the argon matrix with a small amount of acetonitrile shows two separate emission bands, which are attributed not to LE and ICT but to two ICT states with different molecular structures.

From a study of the absorption spectra of a series of *N*-phenylpyrroles with *p*-substituted phenyl groups, it was concluded that the longest wavelength absorption band of PP is connected with a charge transfer from the pyrrole to the phenyl group.[19] In fact, the charge transfer direction switches around, as also concluded from the reversal of the direction of the dipole moment from −1.39 D[3,20] (phenyl to pyrrole) in S_0 to 1.9 D[5] (pyrrole to phenyl) for LE. On the basis of NMR spectra, it was reported that the interaction between the pyrrole nitrogen and the phenyl ring in PP is essentially inductive.[12]

Several theoretical studies are present in the literature which all come to the conclusion that the phenyl and pyrrole groups of PP in the ICT state have a mutually perpendicular conformation.[21−23] By using multiconfigurational second-order perturbation theory (the CASPT2 method), excitation and emission energies as well as molecular geometries (bond distances and angles) in S_0 and several excited states were computed.[21] The twist angle between the phenyl and pyrrole parts of PP was found to decrease upon excitation, from 41.4° in S_0 to 25.5° in S_1, ruling out either planar or perpendicular equilibrium structures in both states. These results are consistent with the experimental data for jet-cooled PP mentioned above.[15] The order of the calculated barrier heights to the planar (9.73 kJ/mol) and perpendicular (6.20 kJ/mol) conformations in S_0 is, however, opposite to the experimental values[15] of 5.47 and 8.96 kJ/mol, respectively. For the LE state, the computed barriers of 5.16 kJ/mol (coplanar) and 26.75 kJ/mol (90°) show the same trend as the experimental data (1.26 and 18.26 kJ/mol),[15] indicating that PP becomes more rigid to twist upon excitation to S_1.

From the calculations,[21] it was further concluded that the broad and structureless lowest-energy absorption band of PP in the gas phase and also in solution has a composite character: a weak LE band (S_1) and a more strongly allowed transition (S_2). In addition, by applying a self-consistent reaction field

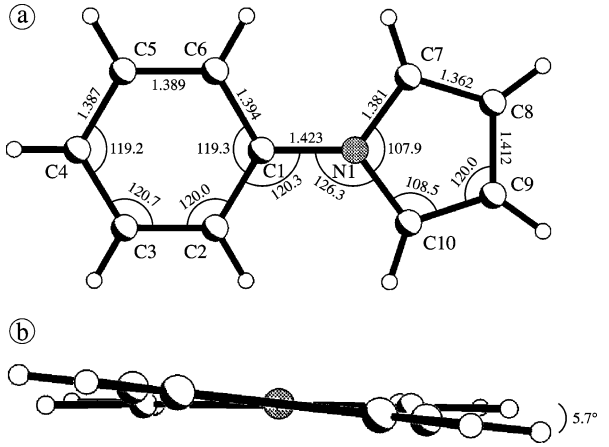

Figure 1. (a) Crystal structure of *N*-phenylpyrrole (PP) determined from X-ray structure analysis at −143 °C. The bond lengths are given in Å (1 Å = 100 pm). Chemically equivalent bond distances and angles were merged. (b) View along the long axis of PP from the pyrrole moiety to the benzonitrile subgroup. A twist angle θ of 5.7° between the phenyl and pyrrole planes is indicated.

treatment (external continuum around a spherical cavity) to the gas phase energies, it was found that in MeCN a TICT state drops down below LE, taken as an explanation for the onset of dual fluorescence with PP in this strongly polar solvent.

Recently, two other theoretical treatments of PP have appeared, based on the DFT/MRCI[22] and CAS/DZV[23] methods. All three treatments[21−23] agree that the phenyl and pyrrole groups of PP are twisted in the ground state (between 36.8 and 44.7°) and that the phenyl ring is much less quinoidal than 4-(dimethylamino)benzonitrile (DMABN), with a bond length ratio (C1−C2)/(C2−C3) (see Figure 1) between 0.996 and 0.998 in S_0 (PP), as compared with the experimental ratio of 0.979 obtained[24] for DMABN. This means that the phenyl and pyrrole moieties in PP are much less strongly coupled than the dimethylamino and benzonitrile groups in DMABN, in accordance with the longer *N*-phenyl bond calculated for PP (1.40−1.42 Å) than that measured for DMABN (1.365 Å),[24] having a value[25] between that of a single bond (1.47 Å, CH_3-NH_2) and a double bond (1.28 Å, oximes and imines).

In all calculations,[21−23] the LE state was found to be planar or more planar than the ground state, increasing in energy when the twist angle becomes larger. Differences are found, however, for the ICT state of PP in the gas phase, with the lowest value for either the coplanar[23] or perpendicular[22] conformation. Merchán et al.[21] did not treat the difference between a perpendicular and a coplanar structure, as calculations for a planar ICT state were not presented. Irrespective of the situation in the gas phase, it is found that a TICT state can become energetically lower than LE in a strongly polar solvent such as MeCN, as this state has the largest calculated gas phase dipole moment and therefore undergoes the largest stabilization by the reaction field. It was stated that the S_1 hypersurface from the twisted to the perpendicular structure has no energy barrier in polar solvents.[21] If that would be the case, then it is not understandable that mainly LE emission is observed with PP in MeCN.[1,2,4−6]

From molecular dynamics simulations of the time-resolved LE and ICT fluorescence of PP in MeCN, it was found that the ICT state, taken to have a structure with mutually perpendicular pyrrole and phenyl groups, is formed in 5−10 ps.[26] It is assumed that the ICT reaction takes place by a damping action of the solvent on PP relaxing on a potential surface without a barrier between LE and ICT,[21] as mentioned above. In the present

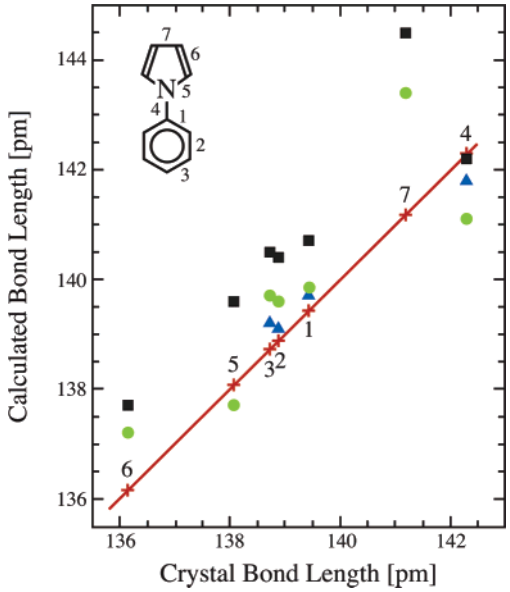

Figure 2. Plot of the calculated bond lengths of *N*-phenylpyrrole (PP), taken from refs 21 (●green), 22 (▲blue), and 23 (■black), versus those obtained from X-ray crystal structure analysis. The red line in the figure represents the equality of calculated and experimental bond lengths. The numbers at the data points refer to the bonds in the molecular structure of PP.

paper, the kinetics and thermodynamics of PP in alkyl cyanides are studied by photostationary and time-resolved measurements as a function of temperature.

Experimental Section

The compounds *N*-phenylpyrrole (PP, from Aldrich), *N*-(4-methylphenyl)pyrrole (PP4M, Aldrich), *N*-(4-methoxyphenyl)-pyrrole (PP4MO, Aldrich), and *N*-(4-cyanophenyl)pyrrole (PP4C, Maybridge) were purified by column chromatography (Al_2O_3), with HPLC as the last purification step. *n*-Hexane, *n*-heptane, and methanol (Merck, Uvasol) were used as received. The solvents perfluoromethylcyclohexane (pFMCH, Bristol Organics), di(*n*-butyl) ether (Aldrich, anhydrous 99.5%), diethyl ether (Merck, Uvasol), tetrahydrofuran (Merck, Uvasol), 1,2-dichloroethane (Merck, reinst), *n*-butyl cyanide (BuCN, Fluka, pure), *n*-propyl cyanide (PrCN, Merck, for analysis), ethyl cyanide (EtCN, Merck, for analysis), acetonitrile (MeCN, Merck, Uvasol), *n*-propanol (Aldrich, for spectroscopy), and ethanol (Merck, Uvasol) were chromatographed over Al_2O_3 just prior to use. The solutions, with an optical density between 0.4 and 0.6 for the maximum of the first band in the absorption spectrum, were deaerated by bubbling with nitrogen for 15 min.

The fluorescence spectra were measured with a quantum-corrected Shimadzu RF-5000PC, Fluoromax 3 or ISA-SPEX Fluorolog 3-22 spectrofluorometer. The excitation spectra (Figure 5a) are not corrected for the spectral response of the reference photodiode. Fluorescence quantum yields Φ_f, with an estimated reproducibility of 2%, were determined with quinine sulfate in 1.0 N H_2SO_4 as a standard[27] ($\Phi_f = 0.546$ at 25 °C). A correction of Φ_f for the difference in refractive index *n* between the solvent and the aqueous sulfuric acid solution is not made.

The triplet yields Φ(ISC) of PP and PP4M, with an estimated accuracy of 10%, were measured by laser flash photolysis using energy transfer to anthracene (T−T absorption spectra in the Supporting Information).[28] A frequency-quadrupled Nd:YAG laser (Continuum Surelight) was employed for excitation at 266 nm. The transient absorption signal was detected in the

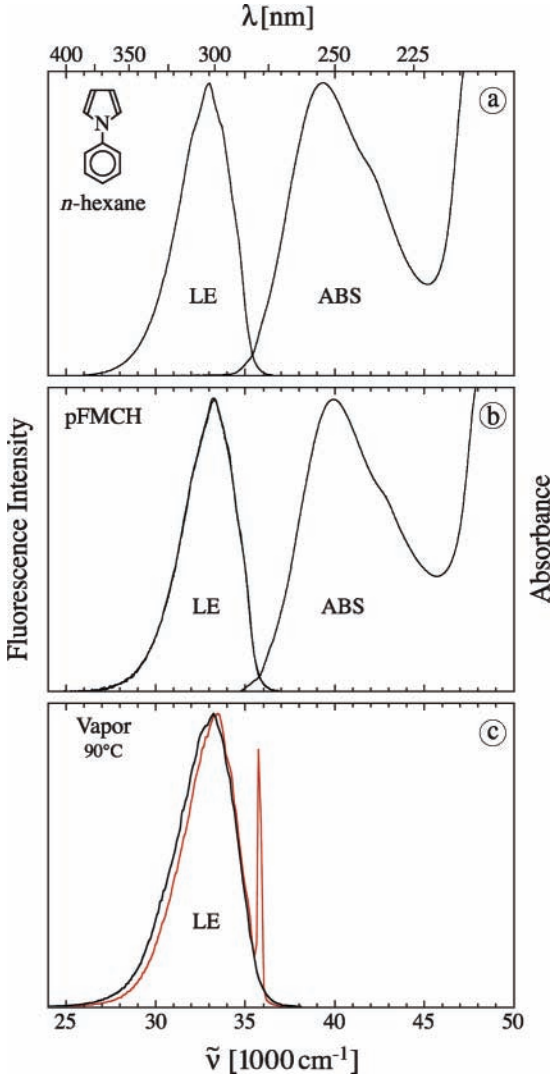

Figure 3. Fluorescence (from the locally excited (LE) state) and absorption (ABS) spectra of *N*-phenylpyrrole (PP) in (a) *n*-hexane at 25 °C, (b) perfluoromethylcyclohexane (pFMCH) at 25 °C, and (c) the vapor phase at 90 °C. Excitation wavelength λ(exc): 260 nm. For the red LE fluorescence spectrum in part c, λ(exc) = 280 nm.

maximum (422 nm) of the T−T absorption spectrum of anthracene, using an experimental setup described previously.[29] Φ(ISC) of the standards is as follows: 1.00 for benzophenone in acetonitrile,[30] 0.96 for *N*-methyl-1,8-naphthanilimide in diethyl ether,[30] and 0.96 for *N*-methyl-phenanthridinone in *n*-hexane.[29] Because of the long fluorescence lifetime and relatively large fluorescence yields of PP and PP4M, the effect of Förster energy transfer and reabsorption of the fluorescence of the target molecules by anthracene was corrected on the basis of lifetime measurements in the presence and absence of the anthracene quencher, as well as by taking into account the anthracene fluorescence intensities in the different samples. The overall corrections were in the range 5−15%.

The fluorescence decay times were determined with a picosecond single photon counting (SPC) system (excitation wavelength λ_{exc}: 276 nm), consisting of a mode-locked titanium-sapphire laser (Coherent, MIRA 900-F) pumped by an argon-ion laser (Coherent, Innova 415).[31] The instrument response function has a half-width of around 18 ps. In addition, a nanosecond (λ_{exc}: 276 nm, deuterium) flashlamp SPC setup was used. The analysis procedure of the fluorescence decays has been described previously.[32,33]

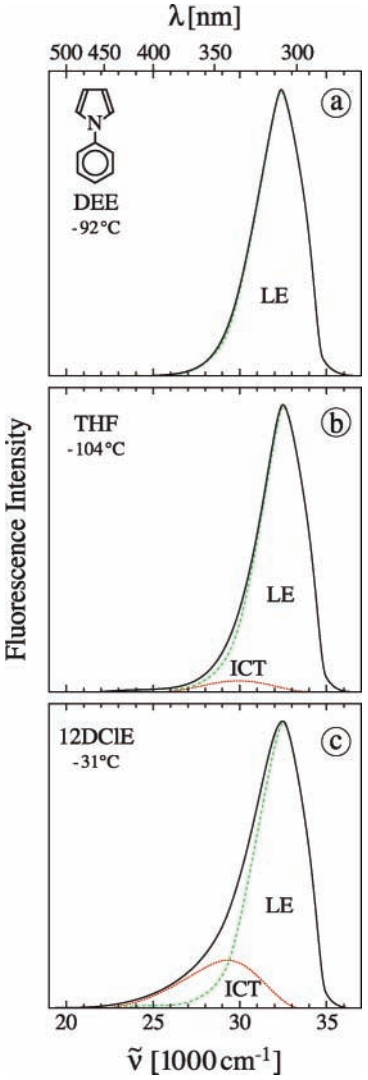

Figure 4. Fluorescence spectra of *N*-phenylpyrrole (PP) in (a) diethyl ether (DEE) at −92 °C, (b) tetrahydrofuran (THF) at −104 °C, and (c) 1,2-dichloroethane (12DClE) at −31 °C. The total fluorescence spectrum in parts b and c has been separated into contributions from the LE and ICT states by spectral subtraction with the fluorescence spectrum of *N*-(4-methylphenyl)pyrrole (PP4M). See the text. Excitation wavelength: ∼265 nm.

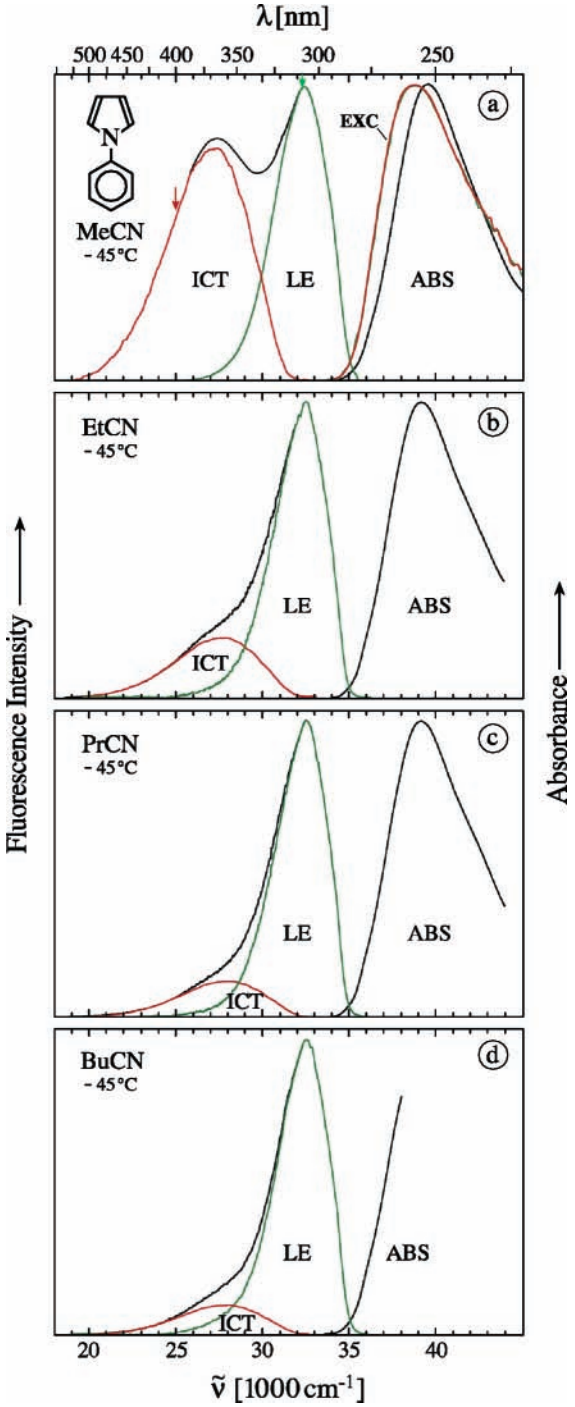

Figure 5. Fluorescence spectra of *N*-phenylpyrrole (PP) at −45 °C in (a) acetonitrile (MeCN), (b) ethyl cyanide (EtCN), (c) *n*-propyl cyanide (PrCN), and (d) *n*-butyl cyanide (BuCN). The total fluorescence spectrum has been separated into contributions from the LE and ICT states by spectral subtraction with the fluorescence spectrum of *N*-(4-methylphenyl)pyrrole (PP4M). See the text. Excitation wavelength: ∼265 nm. The excitation spectrum of PP in MeCN (a) measured at 400 nm (red arrow) is indicated by EXC, which differs from the absorption spectrum because of the absence of correction for the excitation light intensity.

Results and Discussion

Molecular Structure of PP. Comparison with Calculated Ground State Structures. The molecular structure of PP was determined by X-ray analysis (Figure 1). The bond lengths, the twist angle θ and the sum ΣN of bond angles around the amino nitrogen N(1) are collected in Table 1. The pyrrole group of crystalline PP is twisted over an angle θ of 5.7° relative to the plane of the phenyl ring. The *N*-phenyl bond N(1)−C(4) (1.423 Å) is clearly longer than that of DMABN (1.365 Å)[24] and even longer than that of 3,5-dimethyl-4-(dimethylamino)benzonitrile (MMD), with an *N*-phenyl bond length of 1.41 Å and an amino twist angle of 59°, which partly decouples the amino and phenyl groups.[24] The amino nitrogen in PP is planar, as derived from the sum $\Sigma N = 360.0°$. For DMABN crystals, $\Sigma N = 358.8°$, leading to a pyramidality angle between the planes of the dimethylamino group and the phenyl ring of 11−12°, whereas ΣN equals 357.5° for crystalline DIABN.[24,34]

In Figure 2, a comparison is made between the bond lengths determined for crystalline PP by X-ray analysis and the corresponding data coming from calculations reported in the literature (Table 1).[21−23] It is seen that the experimental bond lengths tend to be shorter than those obtained by the theoretical methods, especially for C8−C9 in the pyrrole ring, whereas only the C7−C8 and C9−C10 distances in this ring are calculated to be shorter than those in the crystal (qualitative difference mainly for the pyrrole ring of PP). It is not clear at present what the photophysical significance of these differences

TABLE 1: Bond Distances (in pm, = 0.01 Å) and Structural Parameters of *N*-Phenylpyrrole (PP) from X-ray Data (Crystal) and from Calculations Taken from the Literature[a]

bond (Figure 1)	crystal[b]	ref 21	ref 22	ref 23
C1−N1	142.30(18)	141.1	141.8	142.2
C1−C2	139.37(18)	139.9	139.7	140.7
C2−C3	138.9(2)	139.6	139.1	140.4
C3−C4	138.76(19)	139.7	139.2	140.5
C4−C5	138.7(2)	139.7	139.2	140.5
C5−C6	138.88(19)	139.6	139.1	140.4
C1−C6	139.50(17)	139.9	139.7	140.7
N1−C7	137.91(18)	137.7		139.6
C7−C8	136.2(2)	137.2		137.7
C8−C9	141.2(2)	143.4		144.5
C9−C10	136.1(2)	137.2		137.7
N1−C10	138.25(16)	137.7		139.6
twist angle θ (deg)[c]	5.7	41.1	36.8	40.5
ΣN (deg)[d]	360.0	360.0		

[a] See Figures 1 and 2 and the additional crystallographic data in the Supporting Information. [b] Standard deviation in parentheses. [c] Angle θ between the phenyl and pyrrole planes. [d] Sum of the angles around the nitrogen atom N(1); see Figure 1.

is with respect to the different methodologies and assumptions employed in the calculations.

Absorption Spectra of PP. The absorption spectrum of PP in *n*-hexane and perfluoromethylcyclohexane (pFMCH) (Figure 3a and b) consists of a broad and structureless band, with a maximum $\tilde{\nu}^{max}$(abs) at 39 310 cm^{-1} (254.4 nm) in *n*-hexane and 39 890 cm^{-1} (250.7 nm) in pFMCH; see Table 2. At the low-energy side of the spectrum, a weak structured band can be seen, that may be ascribed to the S_1 state identified by calculations.[21−23] Such a weak structured S_1 band is also observed with DMABN in nonpolar solvents.[35−37] The absorption spectrum obtained with PP in the vapor phase[4,15] has a similar structure, although with a less pronounced S_1 band.

The lowest-energy absorption maximum $\tilde{\nu}^{max}$(abs) of PP undergoes a red shift of 1350 cm^{-1} from the gas phase (40 600 cm^{-1}),[4] via pFMCH (39 890 cm^{-1}) to *n*-heptane (39 250 cm^{-1}); see Table 2. In these nonpolar media, for which the refractive index *n* increases from 1 (gas phase), via 1.279 (pFMCH) to 1.385 (*n*-heptane),[5,38] the polarizability is the determining solvation property.[37,39] Upon an increase in the solvent polarity (Table 2), an unusual[7,34,39−41] shift to higher energies of the absorption maximum $\tilde{\nu}^{max}$(abs) of PP sets in, from 39 190 to 39 420 cm^{-1} for the dialkyl ethers (230 cm^{-1}, di(*n*-butyl) ether to diethyl ether), from 39 320 to 39 580 cm^{-1} for the alkyl cyanides (260 cm^{-1}, PrCN to MeCN), and from 39 420 to 39 500 cm^{-1} for the alcohols (80 cm^{-1}, *n*-propanol to methanol). This small but significant atypical shift to higher energies must mean that only a correspondingly minor change (small decrease) in dipole moment takes place during the absorption process to the Franck−Condon LE state. A similar observation is made with the absorption spectra of PP4M and PP4C (see Table 5 in the Supporting Information), which shows that the phenomenon is not related to a switch of the direction of the dipole moment between S_0 and S_1, as this reversal does not occur for PP4C.[5] In the case of DMABN, in contrast, a red-shift of 1400 cm^{-1} is observed for $\tilde{\nu}^{max}$(abs) when going from *n*-hexane to MeCN.[42] The fluorescence maximum $\tilde{\nu}^{max}$(LE) of PP shifts to lower energies between the gas phase and *n*-hexane (Figure 3) and continues to do so down to the polar solvents MeCN and methanol (Table 2). A similar more or less continuous decrease is found for the energy $E(S_1)$ from 36 030 cm^{-1} (vapor) to 35 250 cm^{-1} (methanol) (Table 2).

Fluorescence Spectra of PP in *n*-Hexane, Diethyl Ether, Tetrahydrofuran, and 1,2-Dichloroethane. In the fluorescence spectrum of PP in the nonpolar solvent *n*-hexane at room temperature, only a single emission from the LE state is observed.[1,2,4,5] The occurrence of dual fluorescence cannot be detected, down to the melting point of the solvent at −95 °C. A similar observation is made with PP in the weakly polar solvent diethyl ether between 25 and −116 °C ($\epsilon^{25} = 4.24$, $\epsilon^{-92} = 8.92$, and $\epsilon^{-116} = 11.7$);[43,44] see Figure 4a.

With PP in tetrahydrofuran ($\epsilon^{25} = 7.39$ and $\epsilon^{-104} = 14.2$),[43,44] a weak incipient ICT fluorescence can be detected at 25 °C, with an ICT/LE fluorescence intensity ratio Φ'(ICT)/Φ(LE) of 0.02, which increases to 0.05 at −104 °C (Figure 4b) because of the larger polarity of the solvent at this temperature. In the more polar 1,2-dichloroethane ($\epsilon^{25} = 10.4$ and $\epsilon^{-31} = 14.7$),[43,44] dual fluorescence then clearly appears, especially upon lowering the temperature, with Φ'(ICT)/Φ(LE) increasing from 0.10 at 25 °C to 0.25 at −31 °C (Figure 4c). These observations indicate that the ICT formation with PP is enhanced when the solvent

TABLE 2: Extinction Coefficients, Absorption Maxima $\tilde{\nu}^{max}$(abs), Fluorescence Maxima $\tilde{\nu}^{max}$(LE) and $\tilde{\nu}^{max}$(ICT), Energy of the S_1 State $E(S_1)$, and Total Fluorescence Quantum Yield Φ_f for *N*-Phenylpyrrole (PP) in Various Solvents at 25 °C

solvent	$f(\epsilon) - {}^1/_2 f(n^2)$[a]	extinction coeff (M^{-1} cm^{-1})	$\tilde{\nu}^{max}$(abs) (1000 cm^{-1})	$\tilde{\nu}^{max}$(LE) (1000 cm^{-1})	$\tilde{\nu}^{max}$(ICT) (1000 cm^{-1})	$E(S_1)$[b] (1000 cm^{-1})	Φ_f
gas phase	0		40.60[c]	33.10[d] (33.41)[d]		36.03[e]	
pFMCH[f]	0.028		39.89	33.24		35.76	0.078
n-hexane	0.000	13 910	39.31	32.97		35.41	0.194
n-heptane	−0.001		39.25	32.90		35.33	
di(*n*-butyl) ether	0.191		39.19	32.79		35.24	
diethyl ether	0.252		39.42	32.76		35.29	0.213
tetrahydrofuran	0.307		39.15	32.66		35.14	0.195
1,2-dichloroethane	0.326		39.31	32.52		35.14	
BuCN[g]	0.366			32.75	29.14	35.15[h]	
PrCN[i]	0.375	13 320	39.32	32.61	28.85	35.19	0.163[j]
EtCN[k]	0.383	13 490	39.40	32.41	28.59	35.06	0.141[j]
MeCN[l]	0.393	13 210	39.58	32.67	28.04	35.31	0.106[j]
n-propanol	0.369		39.42	32.65	28.10	35.21	
ethanol	0.380		39.43	32.68	28.40	35.29	
methanol	0.394		39.50	32.64	27.45	35.25	

[a] Solvent polarity parameter: $f(\epsilon) = (\epsilon - 1)/(2\epsilon + 1)$; $f(n^2) = (n^2 - 1)/(2n^2 + 1)$. [b] Crossing of absorption and fluorescence spectra. Due to the overlap of the S_1 and S_2 bands in the absorption spectrum, $E(S_1)$ is an approximation, giving at least an indication of the differences between the S_1 energies of PP in the different solvents. [c] From ref 4. [d] Excitation at 260 or (280) nm; see Figure 3. [e] Estimated from Figure 3b. [f] Perfluoromethylcyclohexane. [g] *n*-Butyl cyanide. [h] Using the absorption spectrum of PP in PrCN fitted to the low-energy part of the absorption spectrum in BuCN, for which $\tilde{\nu}^{max}$(abs) could not be measured. [i] *n*-Propyl cyanide. [j] Sum of the LE and ICT fluorescence quantum yields; see Table 3. [k] Ethyl cyanide. [l] Acetonitrile.

TABLE 3: ICT and LE Fluorescence Quantum Yields Φ′(ICT) and Φ(LE) and Fluorescence Emission Maxima $\tilde{\nu}^{max}$(ICT) and $\tilde{\nu}^{max}$(LE) of *N*-Phenylpyrrole (PP) in Acetonitrile (MeCN), Ethyl Cyanide (EtCN), *n*-Propyl Cyanide (PrCN), and *n*-Butyl Cyanide (BuCN) at 25 and −45 °C

solvent	*T* (°C)	ϵ^a	Φ′(ICT)/Φ(LE)	Φ′(ICT)	Φ(LE)	$\tilde{\nu}^{max}$(ICT) (1000 cm^{-1})	$\tilde{\nu}^{max}$(LE) (1000 cm^{-1})
MeCN	25	36.7	0.418	0.031	0.074	28.04	32.67
	−45	50.2	1.27	0.036	0.029	27.53	32.62
EtCN	25	29.2	0.174	0.021	0.120	28.59	32.41
	−45	39.0	0.36	0.032	0.088	28.03	32.66
PrCN	25	24.1	0.118	0.017	0.146	28.85	32.61
	−45	35.1	0.22	0.030	0.139	28.28	32.63
BuCN	25	19.8	0.087			29.14	32.76
	−45	27.7	0.14			28.58	32.59

[a] Dielectric constant (ref 43).

TABLE 4: Intersystem Crossing Φ(ISC) and Total Fluorescence Φ(fl) Yields of *N*-Phenylpyrrole (PP) and *N*-(4-Methylphenyl)Pyrrole (PP4M) in *n*-Hexane, Diethyl Ether, and Acetonitrile (MeCN) at 25 °C

solvent	ϵ^a		Φ(ISC)	Φ(fl)[b]	Φ(IC)	Φ′(ICT)/Φ(LE)
n-hexane	1.88	PP	0.43	0.194[c]	0.38	0
		PP4M	0.54	0.228[c]	0.23	0
diethyl ether	4.27	PP	0.33	0.213[c]	0.46	0
		PP4M	0.41	0.301[c]	0.29	0
MeCN	36.7	PP	0.74[d]	0.106[d]	0.15[d]	0.418
			0.64 (ICT)	0.031 (ICT)	0.14 (ICT)	
			0.10 (LE)	0.074 (LE)	0.01 (LE)	
		PP4M	0.60	0.361[c]	0.04	0

[a] Dielectric constant (ref 43). [b] Total fluorescence quantum yield. [c] Only LE fluorescence, Φ(LE); for PP, see Table 2 and Figure 3. [d] Total yields from LE and ICT. For Φ(fl) = Φ′(ICT) + Φ(LE), see Table 3.

polarity becomes larger. This is the result of an increase of $-\Delta H$ as well as of a lowering of the ICT activation barrier E_a, as will be shown below.

Fluorescence Spectra of PP in Acetonitrile, Ethyl Cyanide, *n*-Propyl Cyanide, and *n*-Butyl Cyanide. ICT and LE Emission as a Function of Temperature. The fluorescence and absorption spectra of PP were studied as a function of temperature in the alkyl cyanides MeCN, EtCN, PrCN, and BuCN. In the strongly polar solvent MeCN ($\epsilon^{25} = 36.7$),[43] the additional red-shifted ICT fluorescence band clearly increases in importance upon lowering the temperature,[5] with Φ′(ICT)/Φ(LE) increasing from 0.42 at 25 °C to 1.27 at −45 °C.

At −45 °C, the ICT/LE fluorescence quantum yield ratio Φ′(ICT)/Φ(LE) has reached a value of 1.27 (Figure 5 and Table 3). With PP in the other alkyl cyanide solvents, Φ′(ICT)/Φ(LE) is smaller than that in MeCN (Figure 5), because of the decrease in solvent polarity, with the following results at −45 °C (Table 3): 0.36 (EtCN), 0.22 (PrCN), and 0.14 (BuCN). The energy of the band maximum of the ICT emission $\tilde{\nu}^{max}$(ICT) is strongly red-shifted with respect to the maximum of the main fluorescence (LE) band of PP, for example, 28 040 cm^{-1} (ICT) versus 32 670 cm^{-1} (LE) in MeCN at 25 °C;[5] see Table 2. When the solvent polarity becomes smaller, which takes place in the alkyl cyanide series from MeCN to BuCN, as well as with increasing temperature,[43] $\tilde{\nu}^{max}$(ICT) increases: 27 530/28 040 cm^{-1} (MeCN), 28 030/28 590 cm^{-1} (EtCN), 28 280/28 850 cm^{-1} (PrCN), and 28 580/29 140 cm^{-1} (BuCN) at −45 and 25 °C, respectively (Table 3).

Independence of the Fluorescence Spectrum of PP in Acetonitrile on Excitation Wavelength. It has been reported that the fluorescence spectrum of PP changes with excitation wavelength λ_{exc}, with the ratio Φ′(ICT)/Φ(LE) apparently decreasing when λ_{exc} becomes shorter.[4] This wavelength dependence was attributed to the distribution of the *N*-phenyl twist angle of PP in the ground state (see Figure 1), leading with decreasing λ_{exc} to the excitation of more planar isomers of higher energy, which were thought to be the predominant precursors of the LE emission.[4]

For PP in MeCN at 25 °C, we find, however, identical excitation spectra measured between 294 and 220 nm for two different emission wavelengths (310 nm (LE) and 400 nm (ICT), see Figure 5). This is equivalent to saying that the fluorescence spectrum of PP in this solvent does not change over the excitation wavelength range. It is concluded from this absence of excitation wavelength dependence in the low-energy part of the absorption spectrum, a red-edge effect,[45] that the ICT state can only be reached from the equilibrated LE state and not by direct excitation of variously twisted ground state conformers. Support for this conclusion comes from the analysis of the LE and ICT fluorescence decays, as will be discussed in a later section.

Absence of ICT with *N*-(4-Methylphenyl)pyrrole in Acetonitrile and Other Solvents. An LE Model Compound for PP. In the fluorescence spectrum of *N*-(4-methylphenyl)pyrrole (PP4M) in MeCN, the presence of an ICT emission cannot be detected, neither at 25 °C nor at −44 °C, in clear contrast to what was observed for PP.[5] Not surprisingly, dual fluorescence is also absent with PP4M in a series of less polar solvents: EtCN, PrCN, BuCN, diethyl ether, and *n*-hexane.[5] In accordance with this finding, the fluorescence decays of PP4M in acetonitrile and the other solvents employed here are purely single exponential over the entire temperature range investigated. Also, the fluorescence quantum yield of PP4M in MeCN at 25 °C (0.337, Φ(LE)) is larger than that of PP (0.105, Φ′(ICT) + Φ(LE), Tables 2 and 3), due to the absence of an ICT reaction in the case of the former molecule. Similarly, the fluorescence spectrum of PP4MO in MeCN, another PP derivative with an electron donor substituent, consists of a single LE band and the fluorescence decay is likewise single exponential.

The absence of ICT in the case of PP4M is attributed to two causes. First, the energy of the ICT state of PP4M is expected to be larger than that of PP, because of the decrease of the electron affinity (more negative reduction potential $E(A^-/A)$) of the tolyl group as compared with the phenyl group.[46,47] Second, the presence of the methyl substituent in PP4M reduces the energy of the S_1(LE) state by 100 cm^{-1} in *n*-hexane, as seen by comparing the energies of the crossing of the fluorescence and absorption spectra of PP4M and PP. Both factors lead apparently to a positive ΔH value for PP4M under all experimental conditions of the investigations reported here. This conclusion is not surprising, in view of the relatively small $-\Delta H$ values obtained here for PP even in acetonitrile (see below).

Because of the absence of ICT, PP4M can be used (with an appropriate spectral shift) as the model compound for the LE state in the separation of the ICT and LE contributions to the fluorescence spectra of PP. The fluorescence lifetimes of PP4M can be used to represent the lifetime τ_0(LE) of the LE state of PP.

Intersystem Crossing and Internal Conversion Yields of PP and PP4M at 25 °C. Intersystem crossing yields Φ(ISC) were measured for PP and PP4M in the three solvents *n*-hexane, diethyl ether, and MeCN (Table 4). In all cases, triplet formation is an important decay channel for LE, as well as for the ICT state of PP in MeCN. From Φ(ISC) and the total fluorescence quantum yield Φ(fl), the internal conversion yield Φ(IC) is

TABLE 5: Decay Parameters and Rate Constants for the ICT Reaction of *N*-Phenylpyrrole (PP) at −45 °C in *n*-Propyl Cyanide (PrCN), Ethyl Cyanide (EtCN), and Acetonitrile (MeCN) Taken from the Global Analysis of the LE and ICT Fluorescence Decays in Figure 7

solvent	τ_2 (ps)	τ_1 (ns)	A^a	τ_0(LE)^b (ns)	k_a (10^{10} s^{-1})	k_d (10^{10} s^{-1})	k_a/k_d ^{c}	τ'_0(ICT) (ns)	ΔG^d (kJ/mol)
PrCN	31.3	7.38	0.71	11.77	1.33	1.85	0.719	4.86	+0.63
EtCN	15.4	6.41	1.42	11.73	3.88	2.66	1.459	4.87	−0.81
MeCN	8.7	5.88	6.39	11.66	9.92	1.55	6.40	5.46	−3.52

solvent	τ(LC)^e (ps)	$1/(k_d + 1/\tau'_0(\text{ICT}))^f$ (ps)	$\Phi'(\text{ICT})/\Phi(\text{LE})$	$\Phi'(\text{ICT})$	$\Phi(\text{LE})$	$k'_f(\text{ICT})^a$ (10^7 s^{-1})	$k_f(\text{LE})$ (10^7 s^{-1})
PrCN	55.9	53.4	0.22	0.0303	0.139	0.99	3.21
EtCN	38.5	37.3	0.36	0.0320	0.0879	0.83	3.27
MeCN	67.4	63.8	1.23	0.0362	0.0294	0.71	3.65

^{a} Equation 5. ^{b} Fluorescence lifetime of PP4M; see the text. ^{c} $k_a/k_d \sim A$ when $\tau_2 \ll \tau_1$ (ref 52) as derived from eq 5. ^{d} $\Delta G = -RT \ln(k_a/k_d)$. ^{e} Experimental value; see Figure 10. ^{f} See eq 11.

TABLE 6: Thermodynamic Data for the ICT Reaction of *N*-Phenylpyrrole (PP) in Ethyl Cyanide (EtCN) and Acetonitrile (MeCN) Taken from the Arrhenius Plots in Figure 10

solvent	E_a (kJ/mol)	E_d (kJ/mol)	$-\Delta H^a$ (kJ/mol)	$-\Delta H$(SB)^b (kJ/mol)	E(FC)^c (kJ/mol)	$k_a°$ (10^{12} s^{-1})	$k_d°$ (10^{12} s^{-1})	$-\Delta S^d$ (J K^{-1} M^{-1})
EtCN	9.0 ± 0.2	15.7 ± 0.3	6.7 ± 0.2	5.9 ± 0.1	70.7	4.2 ± 0.4	109 ± 17	27 ± 7
MeCN	5.7 ± 0.3	15.7 ± 0.9	10.0 ± 1.1	8.8 ± 0.1	76.9	2.1 ± 0.3	65 ± 31	28 ± 17

^{a} $-\Delta H = E_a - E_d$. ^{b} From the Stevens−Ban plots in Figure 6; see the text. ^{c} $E(\text{FC}) = E(S_1) - \tilde{\nu}^{\max}(\text{ICT}) + \Delta H$; see Table 2. ^{d} $-\Delta S = (\ln(k_a°/k_d°))/R$.

TABLE 7: Data for *N*-Phenylpyrrole (PP), 4-(Dimethylamino)benzonitrile (DMABN), and 4-(Di-*n*-propylamino)benzonitrile (DPrABN) Used for a Comparison of eqs 10 and 10a

	solvent	$-\Delta H$ (kJ/mol)	T (°C)	$1/\tau'_0$(ICT) (10^8 s^{-1})	F^a (10^8 s^{-1})	$F\tau'_0$(ICT)	$k_a\tau_0$(LE)	$k_d\tau'_0$(ICT)^b	k_a/k_d	τ'_0(ICT)/τ_0(LE)
PP	MeCN	10.0	−45	1.83	0.136	0.074	1157	84.6	6.41	0.47
			−20	1.96	0.234	0.119	1541	182.6	3.16	0.44
PP	EtCN	6.7	−45	2.05	0.589	0.287	455.1	129.5	1.46	0.41
			−90	1.72	0.258	0.150	142.7	20.4	3.30	0.47
PP	PrCN	(5.1)^c	−45	2.06	1.196	0.581	156.5	89.9	0.72	0.41
DMABN	toluene	11.6	−45	2.87	1.67	0.582	29.5	16.1	1.58	0.87
			−20	3.23	2.89	0.895	42.6	37.2	0.92	0.80
			20	3.70	6.91	1.87	65.7	121.5	0.40	0.74
DPrABN	toluene	15.0	−45	3.45	0.10	0.030	70.4	1.02	50.2	0.73
			−20	3.57	0.14	0.039	116.1	3.64	23.1	0.72
			20	3.70	0.31	0.084	182.5	14.3	9.43	0.74

^{a} $F = 1/\tau_0(\text{LE})[(k_d + 1/\tau'_0(\text{ICT}))/k_a]$; see eq 10. ^{b} HTL, $k_d\tau'_0(\text{ICT}) \gg 1$; LTL, $k_d\tau'_0(\text{ICT}) \ll 1$. ^{c} From Stevens−Ban plot: $-\Delta H$(SB) (Figure 6).

TABLE 8: Extrapolated Data at 25 °C for *N*-Phenylpyrrole (PP) in Ethyl Cyanide (EtCN) and Acetonitrile (MeCN) from $k_a°$, $k_a°$, E_a, E_d, and τ'_0(ICT)

solvent	τ_2 (ps)	τ_1 (ns)	τ(LC) (ps)	A^a	$\Phi'(\text{ICT})/\Phi(\text{LE})$
EtCN	3.26	5.745	5.1	0.569	0.181
MeCN	3.07	5.153	8.7	1.83	0.425

^{a} Equation 5.

calculated (eq 1). For PP, Φ(IC) is smaller in MeCN than in the other two solvents, due to the competing ICT reaction. The separation of the total yields Φ(ISC) and Φ(IC) into the LE and ICT contributions can only be carried out after the kinetic data (Scheme 1) for PP in MeCN have been determined (Table 9). This will be discussed in the last section of the paper.

$$\Phi(\text{IC}) = 1 - \Phi(\text{fl}) - \Phi(\text{ISC}) \qquad (1)$$

Temperature Dependence of Φ'(ICT)/Φ(LE) of PP. Stevens−Ban Plots. The temperature dependence of the ICT/LE fluorescence quantum yield ratio $\Phi'(\text{ICT})/\Phi(\text{LE})$ of PP in MeCN, EtCN, PrCN, and BuCN is plotted in Figure 6 (Scheme 1 and eq 2). From these Stevens−Ban plots,[48] it is seen that $\Phi'(\text{ICT})/\Phi(\text{LE})$ strongly increases upon cooling. This means that, for ICT with PP in these four alkyl cyanides, the thermal ICT back reaction k_d is much larger than the reciprocal ICT lifetime $1/\tau'_0$(ICT). Such a condition (high-temperature limit (HTL))[49−51] is generally encountered for systems with a relatively small $-\Delta H$ value, such as for DMABN in toluene (7.2 kJ/mol), for which $k_d = 45 \times 10^9$ s^{-1} and $1/\tau'_0(\text{ICT}) = 0.37 \times 10^9$ s^{-1} at 20 °C.[14,52] For this system, even just above the melting point of this solvent at −95 °C, k_d still remains

SCHEME 1

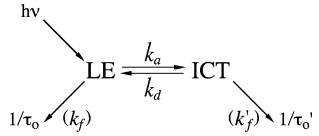

TABLE 9: Extrapolated Experimental Data at 25 °C for *N*-Phenylpyrrole (PP) in Ethyl Cyanide (EtCN) and Acetonitrile (MeCN)

solvent	k_a (10^{11} s^{-1})	k_d (10^{11} s^{-1})	ΔG^a (kJ/mol)	τ_1(LE)^b (ns)	τ(LC) (ps)	τ'_0(ICT) (ns)	τ_0(LE)^c (ns)	$k'_f(\text{ICT})/k_f(\text{LE})^d$	$\Phi'(\text{ICT})/\Phi(\text{LE})^e$
EtCN	1.113	1.953	1.39	5.02		3.20	10.50	0.318	0.174
MeCN	2.11	1.15	−1.50	5.03	9.5	4.02	10.66	0.232	0.418

^{a} $\Delta G = -RT \ln(k_a/k_d)$. ^{b} Experimental longest decay time of the LE fluorescence. ^{c} Fluorescence lifetime of PP4M; see the text. For EtCN, the mean value of τ_0(LE) for MeCN and PrCN is used. ^{d} Extrapolated to 25 °C from the data in Figure 13. ^{e} See Figure 6.

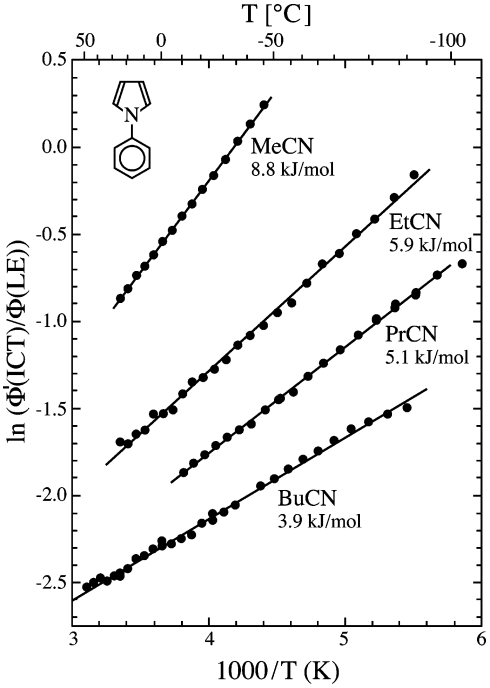

Figure 6. Stevens−Ban plots of the ICT/LE fluorescence quantum yield ratio Φ′(ICT)/Φ(LE) (eq 2) of *N*-phenylpyrrole (PP) in acetonitrile (MeCN), ethyl cyanide (EtCN), *n*-propyl cyanide (PrCN), and *n*-butyl cyanide (BuCN) against the reciprocal absolute temperature. The enthalpy differences $-\Delta H$ (in kilojoules per mole) of the ICT reaction (Scheme 1) calculated from the linear plots are indicated in the figure; see the text.

larger than $1/\tau'_0$(ICT) and the maximum value of Φ′(ICT)/Φ(LE) has therefore not yet been reached, as this occurs in the temperature range where k_d becomes equal to $1/\tau'_0$(ICT).[14,51]

In Scheme 1, k_a and k_d are the rate constants of the forward and backward ICT reaction, τ_0(LE) and τ'_0(ICT) are the fluorescence lifetimes, whereas k_f(LE) and k'_f(ICT) are the radiative rate constants.

$$\Phi'(\mathrm{ICT})/\Phi(\mathrm{LE}) = k'_f(\mathrm{ICT})/k_f(\mathrm{LE})\{k_a/(k_d + 1/\tau'_0(\mathrm{ICT}))\} \quad (2)$$

$$\Phi'(\mathrm{ICT})/\Phi(\mathrm{LE}) = k'_f(\mathrm{ICT})/k_f(\mathrm{LE})\, k_a/k_d \quad (2a)$$

when $k_d \gg 1/\tau'_0$(ICT).

From the plots in Figure 6, it is seen that the high-temperature limit (HTL, $k_d \gg 1/\tau'_0$(ICT), eq 2a)[49−51] holds for PP in all four alkyl cyanide solvents. The following values for the ICT enthalpy difference $-\Delta H$ ($= E_d - E_a$) are obtained from the slopes of the plots: 8.8 kJ/mol (MeCN), 5.9 kJ/mol (EtCN), 5.1 kJ/mol (PrCN), and 3.9 kJ/mol (BuCN); see Table 6. In the calculation of $-\Delta H$, the initial assumption[49,53] is made that the ratio $k'_f(\mathrm{ICT})/k_f(\mathrm{LE})$ does not depend on temperature.[54] A temperature dependence of $k'_f(\mathrm{ICT})/k_f(\mathrm{LE})$ was not expected, as both radiative rate constants were considered to depend on n^2.[49] The absence or presence of a temperature dependence of τ'_0(ICT) does not affect the results found for $-\Delta H$ under HTL conditions (eq 2a). The present approximate data for $-\Delta H$ will be compared in a subsequent section with those calculated directly from the Arrhenius plots of the ICT rate constants k_a and k_d derived from the LE and ICT fluorescence decays of PP measured as a function of temperature.

Time-Resolved Measurements. LE and ICT Picosecond Fluorescence Decays of PP in MeCN, EtCN, and PrCN at −45 °C. The LE and ICT picosecond fluorescence decays of PP in MeCN, EtCN, and PrCN at −45 °C are presented in Figure 7. These LE and ICT decays are measured at wavelengths at which either only LE (292 nm) or only ICT (430 nm) fluorescence occurs; see Figure 5. In the global analysis (LE and ICT from the same experiment) of the LE and ICT decays presented there, double exponential fits lead to good results. The observation that the ICT amplitude ratio A_{21}/A_{22} (eq 4) is close to −1.0 (Figure 7) shows that the ICT state of PP can not be formed by direct excitation from S_0 but originates exclusively from the primarily prepared LE state.[6,7,14]

The decay times τ_1 and τ_2 and the amplitude ratio A resulting from these fits (eqs 3−5) are listed in Table 5. The shortest decay time τ_2 increases in the series MeCN (8.7 ps), EtCN (15.4 ps), and PrCN (31.3 ps), with a corresponding decrease in the amplitude ratio A (eq 5) from 6.39 (MeCN) to 1.42 (EtCN) to 0.71 (PrCN).

$$i_f(\mathrm{LE}) = A_{11}\exp(-t/\tau_1) + A_{12}\exp(-t/\tau_2) \quad (3)$$

$$i_f(\mathrm{ICT}) = A_{21}\exp(-t/\tau_1) + A_{22}\exp(-t/\tau_2) \quad (4)$$

$$A = A_{12}/A_{11} = (k_a + 1/\tau_0(\mathrm{LE}) - 1/\tau_1)/(1/\tau_2 - k_a - 1/\tau_0(\mathrm{LE})) \quad (5)$$

From the decay times τ_2 and τ_1 together with the amplitude ratio A (eqs 3−5) and the lifetime τ_0(LE), the ICT rate constants k_a and k_d and the lifetime τ'_0(ICT) can be determined by using eqs 6−8 (Scheme 1);[6,7,14] see Table 5. The fluorescence lifetime of PP4M in the particular solvent at −45 °C was taken for τ_0(LE), as dual emission is not observed with this system (see above).

$$k_a = (1/\tau_1 + A/\tau_2)/(1 + A) - 1/\tau_0(\mathrm{LE}) \quad (6)$$

$$k_d = \{(1/\tau_2 - 1/\tau_1)^2 - (2k_a + 2/\tau_0(\mathrm{LE}) - 1/\tau_1 - 1/\tau_2)^2\}/4k_a \quad (7)$$

$$1/\tau'_0(\mathrm{ICT}) = 1/\tau_1 + 1/\tau_2 - k_a - k_d - 1/\tau_0(\mathrm{LE}) \quad (8)$$

The radiative rate constants k_f(LE) and k'_f(ICT) can be determined from the separate LE and ICT fluorescence quantum yields Φ(LE) and Φ′(ICT) and the data for k_a, k_d, and τ'_0(ICT) in Table 5 by using eqs 9 and 10. The ratio $k'_f(\mathrm{ICT})/k_f(\mathrm{LE})$ is clearly smaller than unity, as is generally the case for donor/acceptor systems undergoing inter- and intramolecular charge transfer.[13,52,55]

$$k_f(\mathrm{LE}) = \Phi(\mathrm{LE})\{1/\tau_0(\mathrm{LE}) + 1/\tau'_0(\mathrm{ICT})(k_a/(k_d + 1/\tau'_0(\mathrm{ICT}))\} \quad (9)$$

$$k'_f(\mathrm{ICT}) = \Phi'(\mathrm{ICT})\{1/\tau'_0(\mathrm{ICT}) + 1/\tau_0(\mathrm{LE})[(k_d + 1/\tau'_0(\mathrm{ICT}))/k_a]\} = \Phi'(\mathrm{ICT})\{1/\tau'_0(\mathrm{ICT}) + F\} \quad (10)$$

LE/ICT Fluorescence Decays. For systems with two excited states, such as here LE and ICT (Scheme 1), a deconvolution of the ICT fluorescence decay with that of LE as a formal excitation pulse should result in a single decay time τ(LC), which is equal to the sum of the deactivation pathways k_d and $1/\tau'_0$(ICT) starting from the ICT state; see eq 11.[56,57] This is indeed found to be the case for the LE/ICT decays of PP in MeCN and in EtCN at −45 °C. A comparison between the

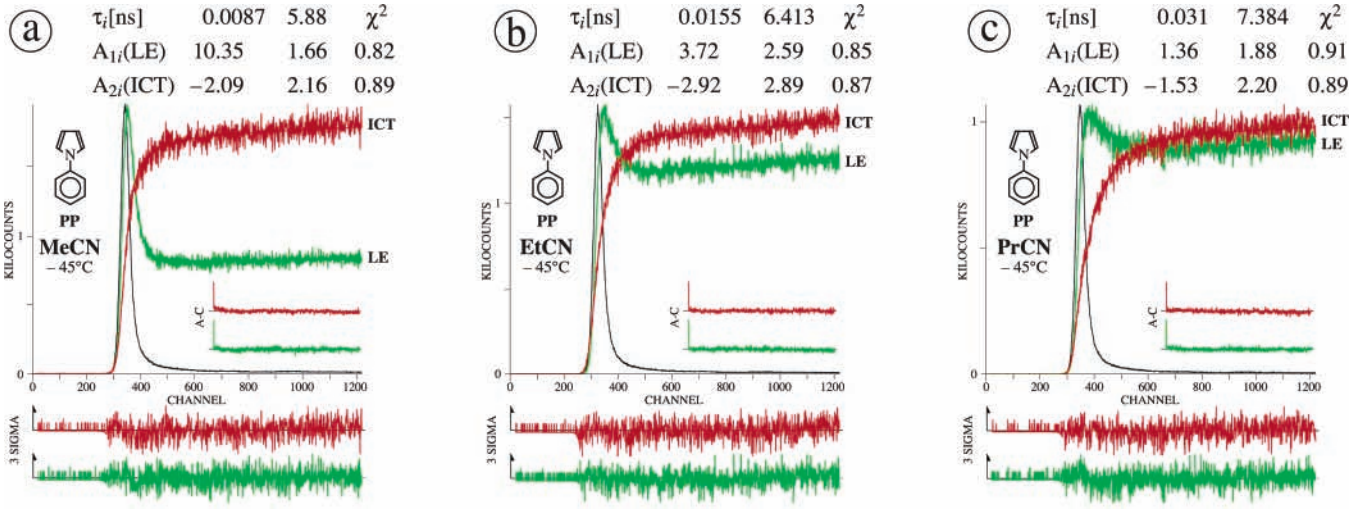

Figure 7. Double exponential LE and ICT fluorescence response functions of *N*-phenylpyrrole (PP) in acetonitrile (MeCN), ethyl cyanide (EtCN), and *n*-propyl cyanide (PrCN) at −45 °C. The LE and ICT decays are analyzed simultaneously (global analysis). The decay times τ_2 and τ_1 and their preexponential factors A_{1i} (LE) and A_{2i} (ICT) are given (eqs 3−5). The shortest decay time τ_2 is listed first. The weighted deviations, expressed in σ (expected deviations), the autocorrelation functions A−C, and the values for χ^2 are also indicated. Excitation wavelength: 276 nm, 0.496 ps/channel. Emission wavelengths: 292 nm (LE); 430 nm (ICT, MeCN and EtCN); and 380 nm (ICT, PrCN).

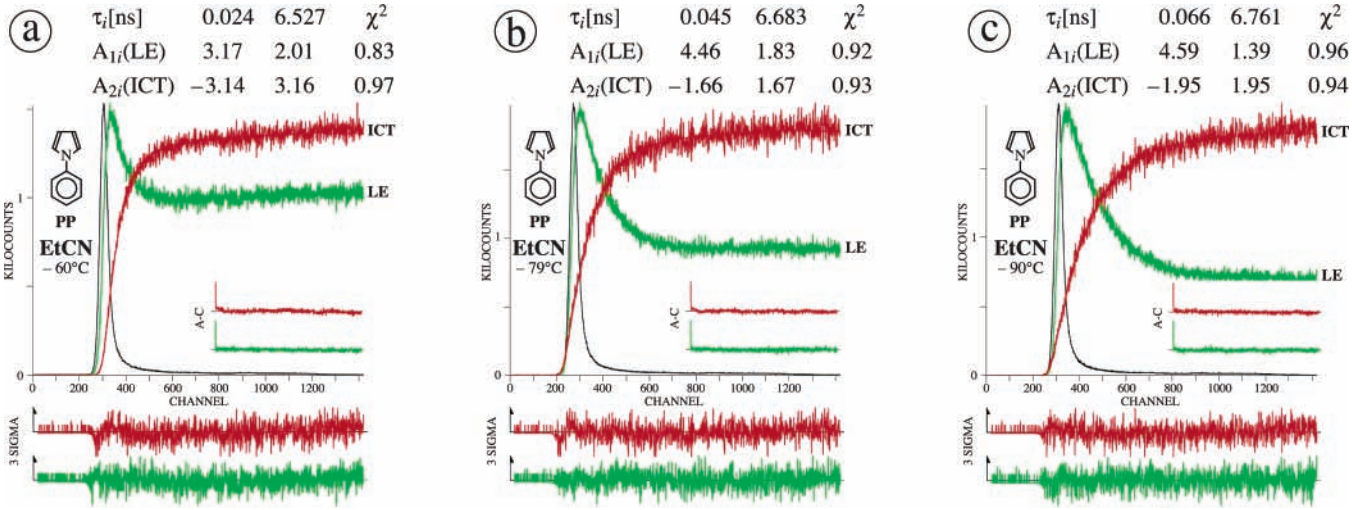

Figure 8. Double exponential LE and ICT fluorescence response functions of *N*-phenylpyrrole (PP) in ethyl cyanide (EtCN) at (a) −70, (b) −79, and (c) −90 °C. The LE and ICT decays are analyzed simultaneously (global analysis). The decay times τ_2 and τ_1 and their preexponential factors A_{1i} (LE) and A_{2i} (ICT) are given (eqs 3−5). The shortest decay time τ_2 is listed first. Excitation wavelength: 276 nm, 0.496 ps/channel. See the caption of Figure 7.

experimental τ(LC) and ($k_d + 1/\tau'_0$(ICT)) values shows that a good agreement is obtained (Table 5).

$$\tau(\mathrm{LC}) = 1/(k_d + 1/\tau'_0(\mathrm{ICT})) \qquad (11)$$

LE and ICT Fluorescence Decays in EtCN and MeCN as a Function of Temperature. LE and ICT fluorescence decays of PP in EtCN were measured as a function of temperature. Examples of a global analysis resulting in double exponential decays are presented in Figure 8. It is seen that the shortest decay time τ_2 increases from 24 ps at −60 °C to 66 ps at −90 °C. Simultaneously, the LE amplitude ratio $A = A_{12}/A_{11}$ ($\cong k_a/k_d$ as $\tau_2 \ll \tau_1$, eqs 3−5)[14,52] becomes larger, from 1.58 to 3.30, indicating that k_a increases in importance with respect to k_d when the temperature is lowered. The ICT amplitude ratio A_{21}/A_{22} (eq 4) equals −1, which shows that the ICT state exclusively originates from the primarily excited LE state.[14,52] The decay time τ_1 undergoes only a small increase with decreasing temperature, from 6.53 ns at −60 °C to 6.76 ns at −90 °C. The overall temperature dependence of τ_2 and A, together with that of τ_1 and τ_0(LE) (fluorescence lifetime of the model compound PP4M, see above), is plotted in Figure 9a.

LE and ICT fluorescence decays were similarly determined for PP in MeCN. An LE and ICT global analysis at −45 °C is shown in Figure 7a. The decay time τ_2 in this solvent increases from 5.9 ps at −20 °C to 8.7 ps at −45 °C, accompanied with a change of A from 3.8 to 6.4 (Figure 9b). Also with PP in EtCN, τ_1 increases slightly upon lowering the temperature: from 5.61 ns at −60 °C to 5.88 ns at −45 °C (Figure 7a and 9b).

Arrhenius Plots of the ICT Rate Constants k_a and k_d of PP in EtCN and MeCN. Thermodynamic Data E_a, E_d, and $-\Delta H$. Temperature Dependence of τ'_0(ICT). From the decay data τ_1, τ_2, and A for PP in EtCN and MeCN, together with the fluorescence lifetime τ_0(LE) of the model compound PP4M in these solvents (Figure 9), the ICT rate constants k_a and k_d and τ'_0(ICT) (Scheme 1) are calculated by employing eqs 6−8. Arrhenius plots of k_a and k_d are shown in parts a and b of Figure 10 for EtCN and MeCN, respectively. From these plots, the

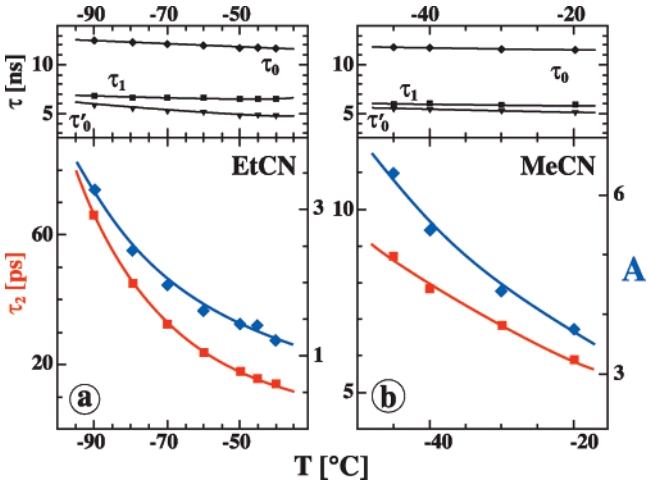

Figure 9. Plots of the fluorescence decay time τ_2 and the amplitude ratio A (bottom) and of the decay time τ_1 and the fluorescence lifetime τ'_0(ICT) for *N*-phenylpyrrole (PP) and of the lifetime τ_0(LE) of *N*-(4-methylphenyl)pyrrole (PP4M) (top) in (a) ethyl cyanide (EtCN) and (b) acetonitrile (MeCN) as a function of temperature. The lines through the data points for τ_2, τ_1, and A are calculated by employing the data for E_a, E_d, k_a^0, and k_d^0 obtained from the Arrhenius plots in Figure 10 (Table 6) together with data for τ'_0(ICT) (eq 8) and τ_0(LE); see the text (eqs 3−5).

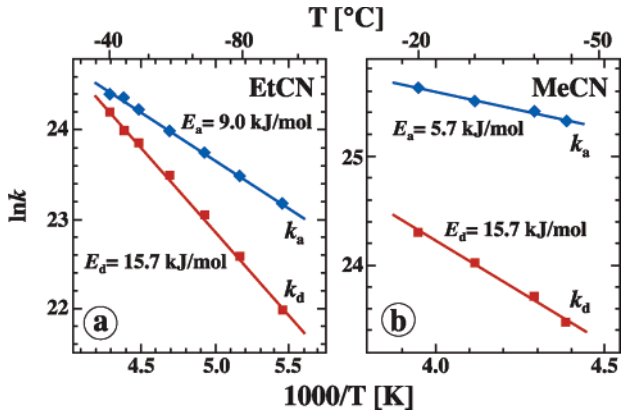

Figure 10. Arrhenius plots of the ICT rate constants k_a and k_d (Scheme 1) of *N*-phenylpyrrole (PP) in (a) ethyl cyanide (EtCN) and (b) acetonitrile (MeCN). The activation energies E_a and E_d (Table 5) are given at each plot. The lines through the data points for k_d and k_d are calculated from the Arrhenius expression $k_i = k_i^0 \exp(E_i/RT)$; see Table 6.

activation energies E_a and E_d of the forward and backward ICT reactions (Scheme 1) are determined, together with their preexponential factors $k_a°$ and $k_d°$. The change in enthalpy ($\Delta H = E_a - E_d$) and also in entropy ($\Delta S = \ln(k_a°/k_d°)/R$) of the ICT reaction can then be obtained from these data. The results are collected in Table 6.

An ICT activation energy E_a of 9 kJ/mol obtained for PP in EtCN clearly shows that the reaction is not barrierless, a condition that has been discussed in the literature for ICT reactions.[58,59] For PP in the more polar solvent MeCN, a somewhat smaller ICT barrier (6 kJ/mol) results, showing that E_a decreases with increasing solvent polarity, in accordance with earlier findings that the activation energy of ICT reactions of DMABN decreases with increasing solvent polarity.[60,61] This observation is an indication that the LE → ICT reaction of PP has a late transition state.[62] The ICT enthalpy change $-\Delta H$ of PP is larger in MeCN (10.3 kJ/mol) than in the less polar solvent EtCN (6.8 kJ/mol), as is to be expected for an ICT reaction.

For the activation energy E_d of the back ICT reaction, the same value (16 kJ/mol) is found in EtCN and in the more polar solvent MeCN. This also indicates that a late transition state is involved in the forward ICT reaction of PP: E_a decreases with solvent polarity in the same manner as $-\Delta H$ (Table 6). Such a late transition state could mean that the ICT reaction with PP is not dominated by changes in the molecular structure such as planarization or twisting of the amino nitrogen, as the sum of the bond angles around this atom is already 360° in the ground state (Figure 1 and Table 1).

The magnitude of the preexponential factors $k_a°$ and $k_d°$ correlates well with that of their corresponding activation energies E_a and E_d. Such a correlation has also been observed for ICT with DMABN and a number of its derivatives,[52] as well as for excimers.[63] The change in entropy $\Delta S = R \ln(k_a°/k_d°)$ calculated for the ICT reaction of PP from these data equals -27 J K^{-1} M^{-1} for EtCN and -31 J K^{-1} M^{-1} for MeCN. These ΔS values are smaller than that of DMABN in toluene (-47 J K^{-1} M^{-1}), a system with a similar $-\Delta H$ value (11.6 kJ/mol).[52] This observation could also be an indication for the absence of dominating structural changes during the ICT reaction. The energy E(FC) of the Franck−Condon state reached by emission from the ICT state of PP, 71 kJ/mol in EtCN and 77 kJ/mol in MeCN, is somewhat larger than that obtained with DMABN and derivatives in toluene (52−68 kJ/mol).[52] The ICT lifetimes τ'_0(ICT) of PP in EtCN and in MeCN (eq 8) are plotted as a function of temperature in parts a and b of Figure 9, respectively. It is seen that τ'_0(ICT) does depend on temperature. In EtCN, τ'_0(ICT) increases from 4.75 ns at −40 °C to 5.97 ns at −90 °C, whereas in MeCN a similar increase from 3.95 ns (−20 °C) to 4.38 ns (−45 °C) takes place.

Influence of Temperature Dependent Solvent Polarity on E_a, E_d, and ΔH. The polarity of the alkyl cyanide solvents in Figure 6 increases upon cooling.[43] Therefore, measurements of E_a, E_d, and ΔH from Φ'(ICT)/Φ(LE) as well as from fluorescence decays do not take place under constant polarity conditions.[52] Since for PP the dipole moment of the ICT state (13 D) is larger than that of the LE state (3 D),[5] $-\Delta H$ will increase upon cooling. Likewise, E_a decreases with increasing solvent polarity,[60,61] and hence with decreasing temperature, in contrast to the assumption of constant activation energies used here. The increase in the dielectric constant ϵ of the already strongly polar alkyl cyanides, from 38.23 (−40 °C) to 46.89 (−90 °C) for EtCN and from 44.50 (−20 °C) to 50.19 (−45 °C) for MeCN, is relatively small, however, so that the thermodynamic data are not influenced to a large extent by the temperature dependence of the solvent polarity.

LE/ICT Decays τ(LC) of PP in EtCN and MeCN as a Function of Temperature. For PP in EtCN as well as in MeCN, the LE/ICT decays are single exponential at all temperatures measured (eq 11). Examples of LE/ICT decays for PP in EtCN at −70, −79, and −90 °C are presented in Figure 11, with times τ(LC) of 97, 157, and 284 ps, respectively. τ(LC) in EtCN ranges from 30.7 ps at −40 °C to 284 ps at −90 °C, whereas in MeCN times τ(LC) between 9.5 ps (25 °C), 29.0 ps (−20 °C), and 67.4 ps (−45 °C) are obtained. The complete set of τ(LC) data in EtCN and MeCN is plotted in Figure 12 and is compared with the corresponding sum ($k_d + 1/(\tau'_0$(ICT))); see eq 11. The good agreement found in this comparison supports the quality of the LE and ICT fluorescence decays and their analysis.

k'_f(ICT) and k_f(LE) as a Function of Temperature. The ICT and LE fluorescence quantum yields Φ'(ICT) and Φ(LE) of PP in EtCN and MeCN were measured as a function of

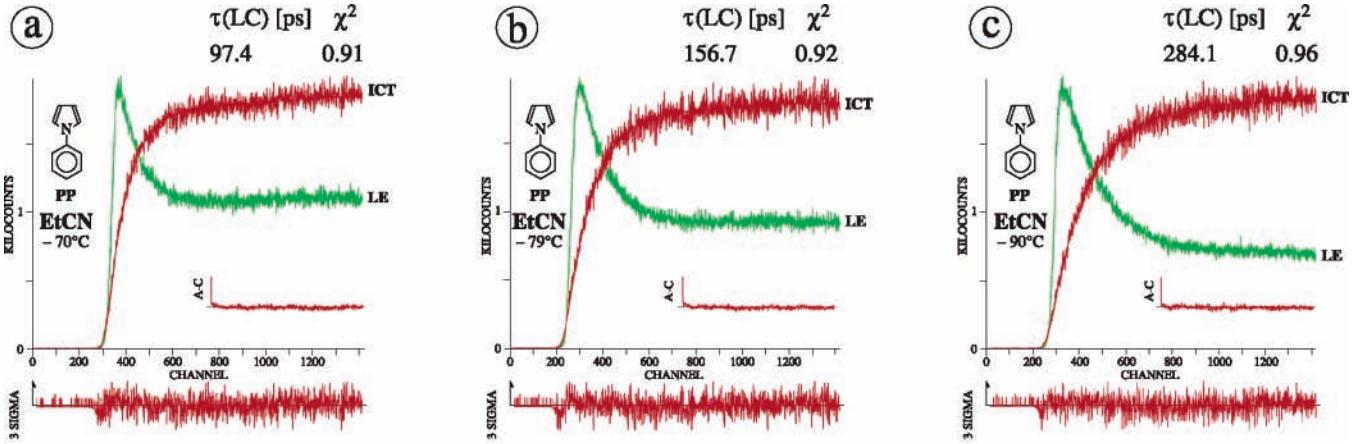

Figure 11. LE/ICT fluorescence decay analysis for *N*-phenylpyrrole (PP) in ethyl cyanide (EtCN) at (a) −70, (b) −79, and (c) −90 °C. The LE decay is used for the deconvolution of the ICT decay, similar to the laser pulse in Figure 8. The decay time τ(LC) should be equal to the sum of k_d and $1/\tau'_0$(ICT) (eq 11), the two processes starting from the ICT state (Scheme 1). Excitation wavelength: 276 nm, 0.496 ps/channel. See the caption of Figure 7.

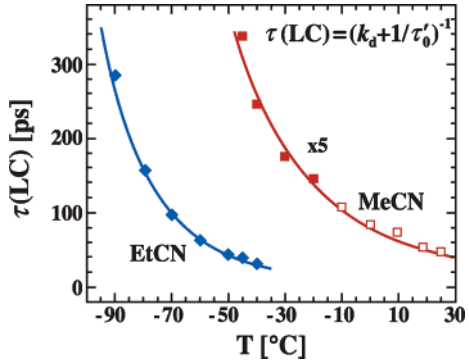

Figure 12. Plot of the experimental LE/ICT decay times τ(LC) of *N*-phenylpyrrole (PP) in ethyl cyanide (EtCN) and acetonitrile (MeCN) versus temperature. The line through the data points represents the expression $1/(k_d + 1/\tau'_0(\text{ICT}))$, eq 11, calculated from the data for k_d^0 and E_d (Table 6) and for τ'_0(ICT), extrapolated from the data points between −45 and −20 °C (Figure 9). The open squares for MeCN represent extrapolated data. See also Figure 11 and Table 8.

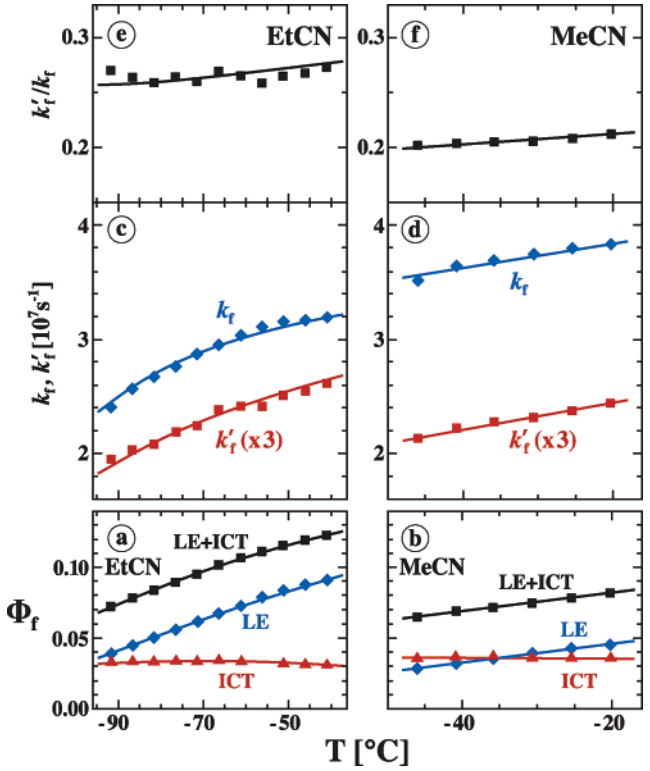

Figure 13. Plots of the fluorescence quantum yields Φ_f and the radiative rate constants k_f(LE) and k'_f(ICT) of *N*-phenylpyrrole (PP) as a function of temperature. The figure consists of three sets of data: the LE and ICT fluorescence quantum yields Φ(LE) and Φ'(ICT) as well as the total fluorescence quantum yield (Φ(LE) + Φ'(ICT)) in (a) ethyl cyanide (EtCN) and (b) acetonitrile (MeCN), the radiative rate constants k_f(LE) and k'_f(ICT) in (c) EtCN and (d) MeCN, and the ratio k'_f(ICT)/k_f(LE) in (e) EtCN and (f) MeCN.

temperature (Figure 13). From these data and k_a, k_d, and τ'_0(ICT) (Figure 9), the ICT and LE radiative rate constants k'_f(ICT) and k_f(LE) are calculated by using eqs 9 and 10. Plots of k_f(LE) and k'_f(ICT) are shown in parts c (EtCN) and d (MeCN) of Figure 13. It is seen that in both solvents the increase of k'_f(ICT) with temperature is not much stronger than that of k_f(LE), which leads to a relatively small positive temperature dependence of k'_f(ICT)/k_f(LE); see Figure 13e and f. As mentioned above in the discussion of the Stevens−Ban (SB) plots for PP in the four alkyl cyanides (Figure 6), this temperature dependence leads to the observed difference between $-\Delta H$ and $-\Delta H$(SB); see Table 6.[51,52] With DMABN in toluene, the increase of k'_f(ICT)/k_f(LE) with temperature is substantially larger than that found here for PP, partly caused by the fact that k_f(LE) decreases with temperature.[37,52]

The temperature dependence of k'_f(ICT) reported for a number of aminobenzonitriles and other dual fluorescent electron donor (D)/acceptor (A)-substituted molecules was interpreted as giving support to the validity of the TICT hypothesis, suggesting a nearly noninteracting radical ion pair $D^+\cdots A^-$ for the structure of the ICT state.[13,55] The experimental data for k'_f(ICT)[13] on which this interpretation was based came, however, from Φ'(ICT) measured as a function of temperature, and the simplified expression (eq 10a) $k'_f(\text{ICT}) = \Phi'(\text{ICT})/\tau'_0(\text{ICT})$ was used instead of the full eq 10 employed here. Such an approximation is not generally valid (see below). Moreover, instead of determining τ'_0(ICT) from an analysis of the LE and ICT fluorescence decays,[52] the ICT lifetime was taken to be constant,[13,55] in conflict with the temperature dependence of k'_f(ICT). This situation will affect the results obtained, especially those for the formal activation energy of k'_f(ICT).[13,54,55]

$$k'_f(\text{ICT}) = \Phi'(\text{ICT})/\tau'_0(\text{ICT}) \qquad (10a)$$

Conditions for the Validity of eq 10a. The simplified equation eq 10a is valid, when $1/\tau'_0(\text{ICT}) \gg F$, where $F =$

$1/\tau_0(\mathrm{LE})[(k_d + 1/\tau'_0(\mathrm{ICT}))/k_a]$; see eq 10 and Scheme 1.[64] This is hence the case when $k_a\tau_0(\mathrm{LE}) \gg (k_d\tau'_0(\mathrm{ICT}) + 1)$. For the high-temperature limit (HTL, $k_d \gg 1/\tau'_0(\mathrm{ICT})$), this condition becomes $k_a\tau_0(\mathrm{LE}) \gg k_d\tau'_0(\mathrm{ICT})$ or $k_a/k_d \gg \tau'_0(\mathrm{ICT})/\tau_0(\mathrm{LE})$, whereas, for the low-temperature limit (LTL, $k_d \ll 1/\tau'_0(\mathrm{ICT})$), the requirement is that $k_a\tau_0(\mathrm{LE}) \gg 1$.[64]

For PP in PrCN at −45 °C (Tables 5 and 7), eq 10a does not hold, as $1/\tau'_0(\mathrm{ICT})$ with $2.06 \times 10^8\ s^{-1}$ is not much larger than F ($1.20 \times 10^8\ s^{-1}$). When going to EtCN and MeCN, F becomes smaller, reaching in MeCN at −45 °C a value of 0.136 and a ratio $F/(1/\tau'_0(\mathrm{ICT}))$ of 0.07, which increases to 0.119 at −20 °C. That the smallest F value is found for PP in MeCN, although the system is under HTL conditions ($k_d\tau'_0(\mathrm{ICT}) \gg 1$), comes from the fact that especially for this system k_a/k_d is clearly larger than $\tau'_0(\mathrm{ICT})/\tau_0(\mathrm{LE})$ (Table 7), which means that the equilibrium is shifted toward the ICT state.[64]

Equation 10a likewise does not hold for DMABN in toluene (Table 7).[52] With this molecule, the same procedure was used for the determination of $k'_f(\mathrm{ICT})$ as that followed here for PP. For 4-(di-*n*-propylamino)benzonitrile (DPrABN) in toluene,[52] $1/\tau'_0(\mathrm{ICT})$ becomes substantially larger than F, although LTL conditions ($k_d\tau'_0(\mathrm{ICT}) \ll 1$) are not reached (Table 7). Also here, F is small because k_a/k_d starts to become clearly larger than $\tau'_0(\mathrm{ICT})/\tau_0(\mathrm{LE})$ as the tempertaure decreases, a consequence of its relatively large $-\Delta H$ value. In the case of DMABN, eq 10a becomes fully applicable in the polar solvents PrCN ($\epsilon^{25} = 24.2$), EtCN ($\epsilon^{25} = 28.3$), or MeCN ($\epsilon^{25} = 36.7$) but not necessarily for data measured in less polar media such as 1-butyl chloride ($\epsilon^{25} = 7.2$),[44] as LTL conditions in this solvent are only reached below −110 °C.[13,55,65]

No Significance of the Temperature Dependence of k'_f(ICT) for ICT Molecular Structure. A temperature dependence of the radiative rate constant, similar to that reported here for $k'_f(\mathrm{ICT})$ as well as $k_f(\mathrm{LE})$ of PP in EtCN and MeCN, has been observed for a number of molecules with small $S_1 \rightarrow S_0$ transition moments. Examples of such systems are DMABN and other dual fluorescent 4-amonobenzonitriles in toluene ($k'_f(\mathrm{ICT})$),[52] intramolecular excimers (1,3-di(2-pyrenyl)propane),[66] exciplexes,[55] and aromatic hydrocarbons with an $S_1(^1L_b)$[49] state, such as pyrene.[66] It is therefore concluded that the temperature dependence of $k'_f(\mathrm{ICT})$ of aminobenzonitriles and other dual fluorescent molecules is not connected with the presence of a perpendicularly twisted TICT state[13,55] but is in fact a natural consequence of the forbidden character of the ICT transition irrespective of its molecular structure, as discussed previously.[67]

Fast ICT with PP in EtCN and MeCN at 25 °C. Conclusion on the ICT Molecular Structure. The rate constant k_a for the LE → ICT reaction of PP at 25 °C, extrapolated from $k_a°$ and E_a (Tables 6 and 8), has a value of $1.1 \times 10^{11}\ s^{-1}$ (EtCN) and $2.1 \times 10^{11}\ s^{-1}$ (MeCN). From these data and those for k_d, $\tau'_0(\mathrm{ICT})$, $\tau_0(\mathrm{LE})$, and $k'_f(\mathrm{ICT})/k_f(\mathrm{LE})$ (Table 6 and Figures 9 and 13), the decay time τ_2 is calculated (Table 8): 3.3 ps (EtCN) and 3.1 ps (MeCN). The experimental LE/ICT decay time $\tau(\mathrm{LC})$ of PP in MeCN at 25 °C (9.5 ps, Figure 12) is in good agreement with the extrapolated $\tau(\mathrm{LC})$ value 8.7 ps (Table 8). A similar agreement is found for $\Phi'(\mathrm{ICT})/\Phi(\mathrm{LE})$.

The fast LE → ICT reaction observed for PP in EtCN and MeCN, with an ICT reaction time $1/k_a$ at 25 °C of 4.7 ps in MeCN and 9.0 ps in EtCN (Table 9), supports our conclusion based on a comparison of PP with the planarized PP derivative fluorazene[6] that the pyrrole and phenyl moieties in the ICT state of PP are coplanar and hence not electronically decoupled, contrary to reports in the literature based on experimental[13] or theoretical[21−23] approaches. It is important to emphasize in this connection that, in discussions of the molecular structure of the ICT state of electron D/A-substituted molecules such as PP and DMABN, the complete absence (the TICT model) or presence (the PICT model) of electronic coupling between the D and A moieties is more significant than focusing the attention primarily[13] on the actual twist angle (90° or zero) between these groups.

Separation of the Overall Yields Φ(ISC) and Φ(IC) into LE and ICT Contributions. On the basis of the data collected in Table 9, the separate LE and ICT contributions to the overall ISC and IC yields Φ(ISC) and Φ(IC) can be determined; see Table 4. From the ISC rate constant $k_{ISC} = \Phi(\mathrm{ISC})/\tau_0$ of the model compound PP4M, a $\Phi^{LE}(\mathrm{ISC})$ value of 0.10 is obtained for PP in MeCN by using an equation similar to eq 9 (rewritten for ISC instead of for fluorescence). In this procedure,[29] the data for k_a, k_d, $\tau'_0(\mathrm{ICT})$, and $\tau_0(\mathrm{LE})$ from Table 9 are employed. The ICT contribution to the ISC yield $\Phi^{ICT}(\mathrm{ISC})$ ($=\Phi(\mathrm{ISC}) - \Phi^{LE}(\mathrm{ISC})$) can be determined from the overall triplet yield Φ(ISC) given in Table 4, resulting in a value of 0.64. The separate LE and ICT yields are derived in a similar manner, giving $\Phi^{LE}(\mathrm{IC}) = 0.01$ and $\Phi^{ICT}(\mathrm{IC}) = 0.14$.

Conclusions

ICT is observed with PP in sufficiently polar solvents, starting with tetrahydrofuran ($\epsilon^{25} = 7.39$). From $\Phi'(\mathrm{ICT})/\Phi(\mathrm{LE})$ measurements over a wide temperature range, under the assumption that $k'_f(\mathrm{ICT})/k_f(\mathrm{LE})$ is temperature independent, approximate thermodynamic data of the ICT reaction are obtained in a series of four alkyl cyanide solvents with decreasing polarity: MeCN ($\epsilon^{25} = 36.7$), EtCN ($\epsilon^{25} = 29.2$), PrCN ($\epsilon^{25} = 24.1$), and BuCN ($\epsilon^{25} = 19.8$). From MeCN to BuCN, $-\Delta H$ decreases as follows: 8.8, 5.9, 5.1, and 3.9 kJ/mol, determined from the accessible high-temperature limit range of the Stevens−Ban plots of $\Phi'(\mathrm{ICT})/\Phi(\mathrm{LE})$.

The LE and ICT fluorescence decays of PP in PrCN, EtCN, and MeCN are double exponential, in accordance with the two-state model (LE and ICT, Scheme 1) employed here. In support of the validity of Scheme 1, the ICT decays deconvoluted with those from LE as the formal excitation pulse are single exponential, which is an indication of the good quality of the data and their analysis. The decay times $\tau(\mathrm{LC})$, so measured, correspond well with the reciprocal of the sum of k_d and $1/\tau'_0(\mathrm{ICT})$ obtained from the separate LE and ICT decay analysis (eq 11). Thermodynamic data for the ICT reaction of PP in MeCN and EtCN are determined from time-resolved fluorescence measurements as a function of temperature. In the less polar solvent EtCN as compared with MeCN, the activation energy E_a of the forward ICT reaction becomes larger (9.0 vs 6.5 kJ/mol). Whereas the ICT reaction enthalpy $-\Delta H$ shows a similar behavior (9.3 vs 6.7 kJ/mol), the activation energy E_d of the back reaction remains practically the same (16 kJ/mol) within experimental accuracy. This indicates that a late transition state governs the LE → ICT reaction of PP in these solvents, as is also seen from the decrease of E_a with solvent polarity.

With PP in EtCN and MeCN, $k'_f(\mathrm{ICT})$ and $k_f(\mathrm{LE})$ increase with temperature. This is caused by the low transition dipole moment of the ICT and LE transition and hence does, in the case of $k'_f(\mathrm{ICT})$, not contain information on the molecular structure (TICT or PICT) of the ICT state.

In MeCN at 25 °C, the extrapolated ICT reaction time $1/k_a$ is 4.7 ps, whereas, in EtCN, $1/k_a$ is 9.0 ps. These results show that with PP in MeCN and EtCN fast ICT takes place, in accordance with our previous interpretation based on a com-

parison of PP with its planarized derivative fluorazene that large amplitude motions do not occur during the reaction to a planar ICT state.

Acknowledgment. The generous support of the Volkswagen Foundation (Project Intra- and Intermolecular Electron Transfer) in the initial stages of the investigations is gratefully acknowledged. A.D. expresses his thanks to the Hungarian Science Foundation (OTKA Project No. T 45890). Mr. J. Bienert, Mr. W. Bosch, and Mr. H. Lesche are thanked for expert technical assistance. N.K. and D.S. acknowledge financial support of the DFG (Grant No. Sta 334/8-2).

Supporting Information Available: Figures showing T−T absorption spectra and the asymmetric unit of PP in two different viewing directions and tables showing crystallographic data, structure refinement data, atomic coordinates, equivalent isotropic displacement parameters, bond lengths and angles, anisotropic displacement parameters, and absorption maxima. This material is available free of charge via the Internet at http://pubs.acs.org.

References and Notes

(1) Rettig, W.; Marschner, F. *Nouv. J. Chim.* **1983**, *7*, 425.
(2) Rettig, W.; Marschner, F. *New J. Chem.* **1990**, *14*, 819.
(3) Lumbroso, H.; Bertin, D. M.; Marschner, F. *J. Mol. Struct.* **1988**, *178*, 187.
(4) Sarkar, A.; Chakravorti, S. *Chem. Phys. Lett.* **1995**, *235*, 195.
(5) Yoshihara, T.; Galievsky, V. A.; Druzhinin, S. I.; Saha, S.; Zachariasse, K. A. *Photochem. Photobiol. Sci.* **2003**, *2*, 342.
(6) Yoshihara, T.; Druzhinin, S. I.; Zachariasse, K. A. *J. Am. Chem. Soc.* **2004**, *126*, 8535.
(7) Zachariasse, K. A.; Druzhinin, S. I.; Bosch, W.; Machinek, R. *J. Am. Chem. Soc.* **2004**, *126*, 1705.
(8) Techert, S.; Zachariasse, K. A. *J. Am. Chem. Soc.* **2004**, *126*, 5593.
(9) This twist angle of 42° was based on a comparison with *N*,*N*-dimethylaniline. A similar value (39°) was obtained from combustion data of PP as compared with aniline (ref 10). In both comparisons, differences in the *N*-phenyl bond lengths and hence the extent of conjugation between the rings may lead to complications.
(10) Schomaker, V.; Pauling, L. *J. Am. Chem. Soc.* **1939**, *61*, 1769.
(11) Fong, C. W. *Aust. J. Chem.* **1980**, *33*, 1763.
(12) Jones, R. A.; Spotswood, T. McL.; Cheuychit, P. *Tetrahedron* **1967**, *23*, 4469.
(13) Grabowski, Z. R.; Rotkiewicz, K.; Rettig, W. *Chem. Rev.* **2003**, *103*, 3899.
(14) Leinhos, U.; Kühnle, W.; Zachariasse, K. A. *J. Phys. Chem.* **1991**, *95*, 2013.
(15) Okuyama, K.; Numata, Y.; Odawara, S.; Suzuka, I. *J. Chem. Phys.* **1998**, *109*, 7185.
(16) Belau, L.; Haas, Y.; Rettig, W. *Chem. Phys. Lett.* **2002**, *364*, 157.
(17) Schweke, D.; Haas, Y. *J. Phys. Chem. A* **2003**, *107*, 9554.
(18) Belau, L.; Haas, Y.; Rettig, W. *J. Phys. Chem. A* **2004**, *108*, 3916.
(19) Matsuo, T.; Shosenji, H.; Miyamoto, R. *Bull. Chem. Soc. Jpn.* **1968**, *41*, 2849.
(20) The minus sign of the dipole moment refers to the opposite direction (phenyl to pyrrole) of the charge transfer in S_0 as compared with the LE and ICT states. See also refs 5 and 17.
(21) Proppe, B.; Merchán, M.; Serrano-Andrés, L. *J. Phys. Chem. A* **2000**, *104*, 1608.
(22) Parusel, A. B. *Phys. Chem. Chem. Phys.* **2000**, *2*, 5545.
(23) Zilberg, S.; Haas, Y. *J. Phys. Chem. A* **2002**, *106*, 1.
(24) Heine, A.; Herbst-Irmer, R.; Stalke, D.; Kühnle, W.; Zachariasse, K. A. *Acta Crystallogr.* **1994**, *B50*, 363.
(25) March, J. *Advanced Organic Chemistry*, 4th ed.; Wiley: New York, 1992; p 21.
(26) Manz, J.; Proppe, B.; Schmidt, B. *Phys. Chem. Chem. Phys.* **2002**, *4*, 1876.
(27) Demas, J. N.; Crosby, G. A. *J. Phys. Chem.* **1971**, *75*, 991.
(28) Grabner, G.; Köhler, G.; Marconi, G.; Monti, S.; Venutti, E. *J. Phys. Chem.* **1990**, *94*, 3609.
(29) Demeter, A.; Bérces, T.; Zachariasse, K. A. *J. Phys. Chem. A* **2001**, *105*, 4611.
(30) Suzuki, K.; Demeter, A.; Kühnle, W.; Tauer, E.; Zachariasse, K. A.; Tobita, S.; Shizuka, H. *Phys. Chem. Chem. Phys.* **2000**, *2*, 981.
(31) Rückert, I.; Demeter, A.; Morawski, O.; Kühnle, W.; Tauer, E.; Zachariasse, K. A. *J. Phys. Chem. A* **1999**, *103*, 1958.
(32) Striker, G. In *Deconvolution and Reconvolution of Analytical Signals*; Bouchy, M., Ed.; University Press: Nancy, France, 1982; p 329.
(33) Zachariasse, K. A.; Kühnle, W.; Leinhos, U.; Reynders, P.; Striker, G. *J. Phys. Chem.* **1991**, *95*, 5476.
(34) Demeter, A.; Druzhinin, S. I.; George, M.; Haselbach, E.; Roulin, J.-L.; Zachariasse, K. A. *Chem. Phys. Lett.* **2000**, *323*, 351.
(35) Zachariasse, K. A.; von der Haar, Th.; Hebecker, A.; Leinhos, U.; Kühnle, W. *Pure Appl. Chem.* **1993**, *65*, 1745.
(36) Zachariasse, K. A.; Grobys, M.; Tauer, E. *Chem. Phys. Lett.* **1997**, *274*, 372.
(37) Druzhinin, S. I.; Demeter, A.; Galievsky, V. A.; Yoshihara, T.; Zachariasse, K. A. *J. Phys. Chem. A* **2003**, *107*, 8075.
(38) Landolt-Börnstein. In *Numerical Data and Functional Relationships in Science and Technology, New Series*; Lechner, M. D., Ed.; Springer: Berlin, 1996; Volume 38B, Group III.
(39) Suppan, P.; Ghoneim, N. *Solvatochromism*; The Royal Society of Chemistry: Cambridge, U.K., 1997.
(40) Lippert, E.; Lüder, W.; Boos, H. In *Advances in Molecular Spectroscopy*; European Conference on Molecular Spectroscopy, Bologna, Italy, 1959; Mangini, A., Ed.; Pergamon: Oxford, U.K., 1962; p 443.
(41) Il'ichev, Yu. V.; Kühnle, W.; Zachariasse, K. A. *Chem. Phys.* **1996**, *211*, 441.
(42) Zachariasse, K. A. Unpublished results.
(43) Landolt-Börnstein. In *Numerical Data and Functional Relationships in Science and Technology, New Series*; Madelung, O., Ed.; Springer: Berlin, 1991; Volume 6, Group IV.
(44) Timmermans, J. *Physico-Chemical Constants of Pure Organic Compounds*; Elsevier: New York, 1950.
(45) Demchenko, A. P. *Luminescence* **2002**, *17*, 19.
(46) The lower electron affinity and more negative reduction potential of toluene as compared with benzene is based on the influence of methyl substituents (electron donor) on the reduction potential of other aromatic hydrocarbons such as naphthalene, anthracene, and pyrene (ref 47).
(47) Koper, C.; Jenneskens, L. W.; Sarobe, M. *Tetrahedron Lett.* **2002**, *43*, 3833.
(48) Stevens, B.; Ban, M. I. *Trans. Faraday Soc.* **1964**, *60*, 1515.
(49) Birks, J. B. *Photophysics of Aromatic Molecules*; Wiley: London, 1970.
(50) Zachariasse, K. A.; Busse, R.; Duveneck, G.; Kühnle, W. *J. Photochem.* **1985**, *28*, 237.
(51) Zachariasse, K. A. *Trends Photochem. Photobiol.* **1994**, *4*, 211.
(52) Il'ichev, Yu. V.; Kühnle, W.; Zachariasse, K. A. *J. Phys. Chem. A* **1998**, *102*, 5670.
(53) Knibbe, H.; Rehm, D.; Weller, A. *Ber. Bunsen-Ges. Phys. Chem.* **1969**, *73*, 839.
(54) When a formal Arrhenius expression is adopted for the radiative rates k_f'(ICT) and k_f(LE), the ratio of the ICT and LE radiative rates can be expressed as $k_f'(\mathrm{ICT})/k_f(\mathrm{LE}) = k_f^\circ(\mathrm{ICT})/k_f^\circ(\mathrm{LE}) \exp(-(E_f(\mathrm{ICT}) - E_f(\mathrm{LE}))/RT)$, where k_f° is the preexponential factor and E_f is the activation energy. The slope of the Stevens−Ban plots under HTL conditions ($k_d \gg \tau'_0(\mathrm{ICT})$), see eqs 2 and 2a, is then equal to $-\Delta H - (E_f(\mathrm{ICT}) - E_f(\mathrm{LE}))$.
(55) Van der Auweraer, M.; Grabowski, Z. R.; Rettig, W. *J. Phys. Chem.* **1991**, *95*, 2083.
(56) Conte, J. C.; Martinho, J. M. G. *Chem. Phys. Lett.* **1987**, *134*, 350.
(57) Zachariasse, K. A.; Yoshihara, T.; Druzhinin, S. I. *J. Phys. Chem. A* **2002**, *106*, 6325. Erratum: *J. Phys. Chem. A* **2002**, *106*, 8978.
(58) Bagchi, B.; Fleming, G. R. *J. Phys. Chem.* **1990**, *94*, 9.
(59) Rettig, W.; Fritz, R.; Braun, D. *J. Phys. Chem. A* **1997**, *101*, 6830.
(60) Hicks, J. M.; Vandersall, M. T.; Sitzmann, E. V.; Eisenthal, K. B. *Chem. Phys. Lett.* **1987**, *135*, 413.
(61) Leinhos, U. Ph.D. Thesis, University of Göttingen, 1991.
(62) Isaacs, N. *Physical Organic Chemistry*, 2nd ed.; Longman: Harlow, U.K., 1995; Chapter 2.
(63) Zachariasse, K. A.; Maçanita, A. L.; Kühnle, W. *J. Phys. Chem. B* **1999**, *103*, 9356.
(64) Under HTL conditions ($k_d \gg 1/\tau'_0(\mathrm{ICT})$), $k'_f(\mathrm{ICT}) = \Phi'(\mathrm{ICT})\{1/\tau'_0(\mathrm{ICT}) + 1/\tau_0(\mathrm{LE})\, k_d/k_a\}$. The simplified equation (eq 10a) $k'_f(\mathrm{ICT}) = \Phi'(\mathrm{ICT})\, 1/\tau'_0(\mathrm{ICT})$ then holds when $1/\tau'_0(\mathrm{ICT}) \gg 1/\tau_0(\mathrm{LE})\, k_d/k_a$ or $k_a/k_d \gg \tau'_0(\mathrm{ICT})/\tau_0(\mathrm{LE})$, together with $k_d \gg 1/\tau'_0(\mathrm{ICT})$ (HTL). This means that eq 10a is valid when k_a/k_d, the equilibrium constant K of the ICT reaction, is much larger than 1, that is, when the equilibrium is strongly shifted towards the ICT state. On the other hand, for an ICT reaction under LTL conditions ($k_d \ll 1/\tau'_0(\mathrm{ICT})$), the conceptually simple situation of an irreversible LE → ICT reaction, eq 10a is generally valid, provided that $k_a \gg 1/\tau_0(\mathrm{LE})$ or $k_a\tau_0(\mathrm{LE}) \gg 1$. It should be noted that the magnitude of the ICT enthalpy difference $-\Delta H$ determines whether HTL (small $-\Delta H$) or LTL (large $-\Delta H$) conditions prevail (refs 50−52). See Table 8.
(65) Rettig, W. *J. Lumin.* **1980**, *26*, 21.
(66) Galievsky, V.; Zachariasse, K. A. Manuscript in preparation.
(67) Zachariasse, K. A. *Chem. Phys. Lett.* **2000**, *320*, 8 and references therein.